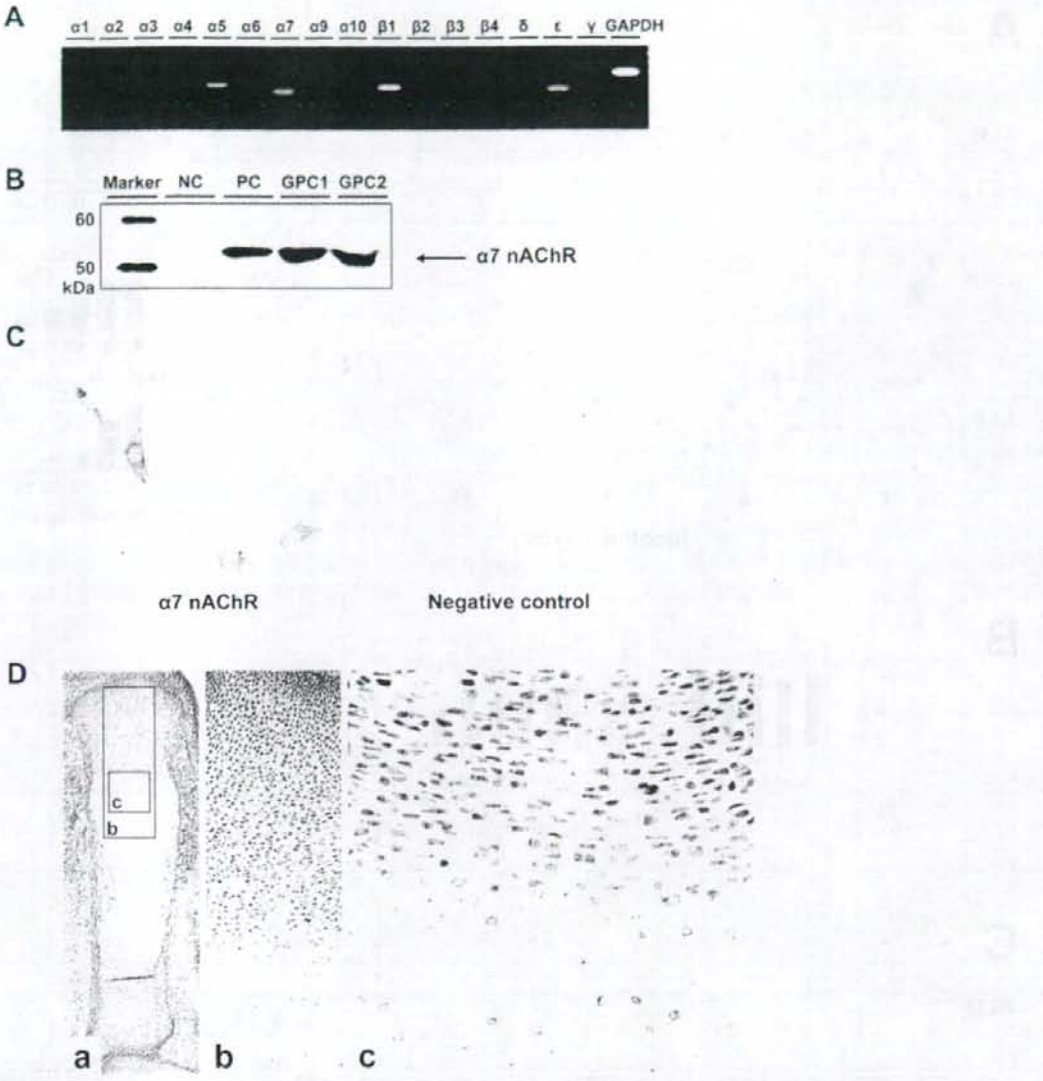

Figure 1. Detection and localization of nAChR subunits in growth plate chondrocytes. A: The expression of each subunit of nAChR. Total RNA was isolated from primary culture of human growth plate chondrocytes. The primers for each subunit are listed in Tables S1–S3. RT-PCR amplified products of alpha5, alpha7, beta1 and epsilon subunits of nAChR and GAPDH. B: Western blot analysis of alpha7 subunit of nAChR in primary chondrocyte cultures. NC: negative control (adipocyte), PC: positive control (PC-12 cell), GPC1,2: human growth plate chondrocyte derived from extra fingers of two individuals. C: Immunocytochemical analysis of alpha7 nAChR subunit in human growth plate chondrocytes. Primary chondrocytes were stained with alpha7 nAChR subunit-specific antibody. D: Immunohistochemical analysis of alpha7 nAChR subunit in tibia of E15.5 fetuses. Alpha7 nAChR are detected at resting, proliferating and pre-hypertrophic chondrocytes of murine growth plate.
doi:10.1371/journal.pone.0003945.g001

of maternal nicotine exposure on skeletal development of murine fetuses in which the alpha7 nAChR gene is disrupted. Maternal genotype is alpha7 nAChR +/− in this experiment (Figure 6), unlike the experiment using wild type mice (Figure 5, maternal genotype: alpha7 nAChR +/+), and littermate fetuses (alpha7 nAChR −/− and alpha7 nAChR +/+) were compared to exclude the effect of nicotine on maternal bodies. Nicotine significantly reduced FL and HL/FL in alpha7 nAChR +/+ fetuses but not in alpha7 nAChR −/− fetuses (Figure 6A, B). However, nicotine did not significantly affect body weight (BW) in both genotypes

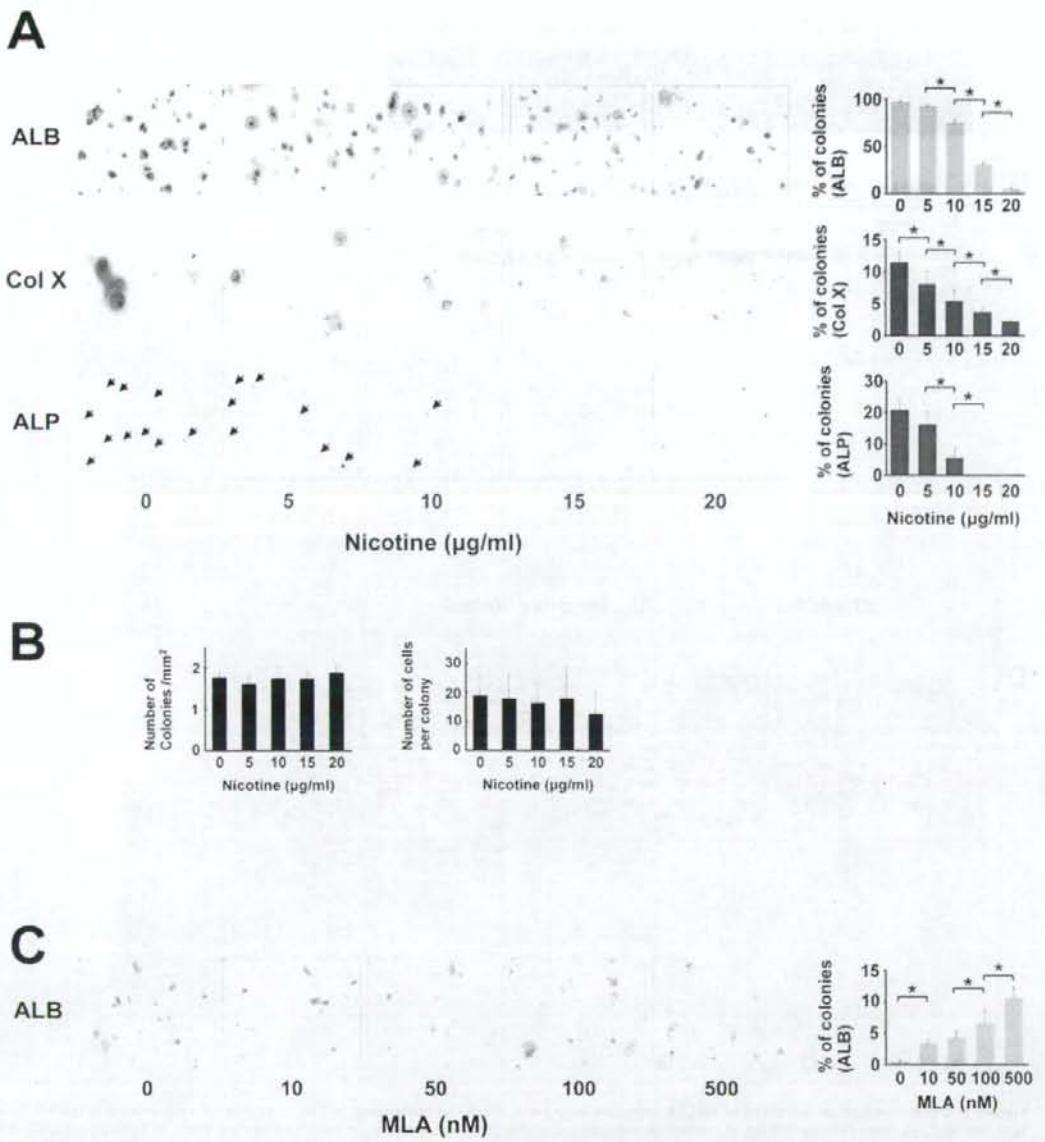

Figure 2. Effect of nicotine on growth plate chondrocytes in agarose gel. Growth plate chondrocytes were cultured in an agarose gel using the modified method previously described [28], and exposed to nicotine and MLA, a specific antagonist for alpha7 nAChR, at the indicated concentration. After three weeks of cultivation, suspension agarose was transferred to a glass slide and the following histological analyses were then performed. A: Microscopic appearance of chondrocyte colonies. From top to bottom: ALB (Alcian blue stain), Col X (immunocytochemistry by an anti-Col X antibody), ALP (enzyme cytochemistry of alkaline phosphatase). For ALB and Col X stain, the slides were counterstained with kernechtrot and hematoxylin, respectively. Percentage of ALB- stained, Col X- positive, and Alkaline phosphatase- positive colonies were counted (right panel, from top to bottom). All the ALP positive colonies in the panels are indicated by arrowheads. Nicotine concentration-dependently suppressed the percentage of the colonies stained with ALB, Col X, and ALP. *, statistically significant, $P<0.02$. B: Number of colonies and number of cells per colony. The number of colonies with a diameter greater than 50 μm (left panel) and cell number per colony (right panel) were counted on the ALB- stained agarose gel slides. C: Microscopic appearance of chondrocyte colonies stained with ALB. MLA reversed the decrease of ALB- positive matrix in a concentration-dependent manner under constant nicotine concentration (20 μg/ml). The percentage of ALB-positive colonies exceeded 10% by using 500 nM MLA. *, statistically significant, $P<0.02$.

doi:10.1371/journal.pone.0003945.g002

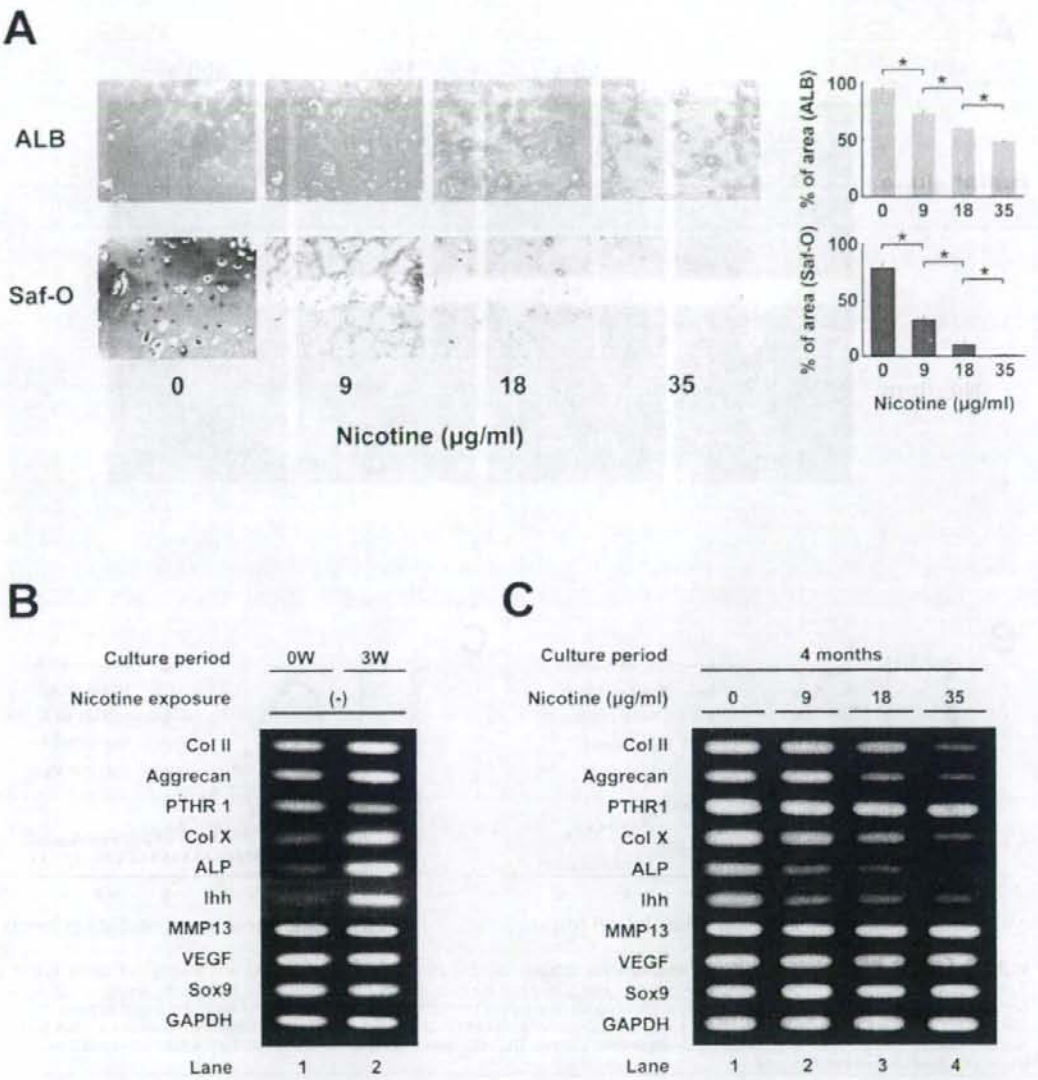

Figure 3. Long-term (four months) effect of nicotine on growth plate chondrocytes in alginate beads. Growth plate chondrocytes in alginate beads were exposed to the indicated concentration of nicotine for four months. A: Microscopic view of chondrocytes in alginate beads after four-months cultivation. Upper panels: ALB stain, lower panels: Safranin-O stain. Chondrocytes were surrounded by matrix which they secreted. Nicotine decreased the area stained with ALB or Safranin-O in a concentration-dependent manner. *, statistically significant, $P<0.02$. B: RT-PCR analysis of chondrocyte-specific gene expression in the chondrocytes at the start of cultivation (lane 1: 0W) and three weeks (lane 2: 3W). From top to bottom: genes for Col II, Aggrecan, parathyroid hormone receptor type 1 (PTHR1), Col X, alkaline phosphatase (ALP), Indian hedgehog (Ihh), matrix metalloproteinase type13 (MMP13), vascular endothelial growth factor (VEGF), Sox9 and GAPDH. C: RT-PCR analysis of chondrocyte-specific gene expression in chondrocytes embedded in alginate beads exposed to the indicated concentration of nicotine for four months. Expression of early stage matrix-gene (Col II and Aggrecan) and markers of hypertrophic chondrocytes (Col X, ALP and Ihh) increased after three weeks of cultivation (B). Nicotine decreased the expression of these genes in a concentration-dependent manner, but had little effect for the expression of MMP13, VEGF, and control genes (Sox9 and GAPDH) (C).
doi:10.1371/journal.pone.0003945.g003

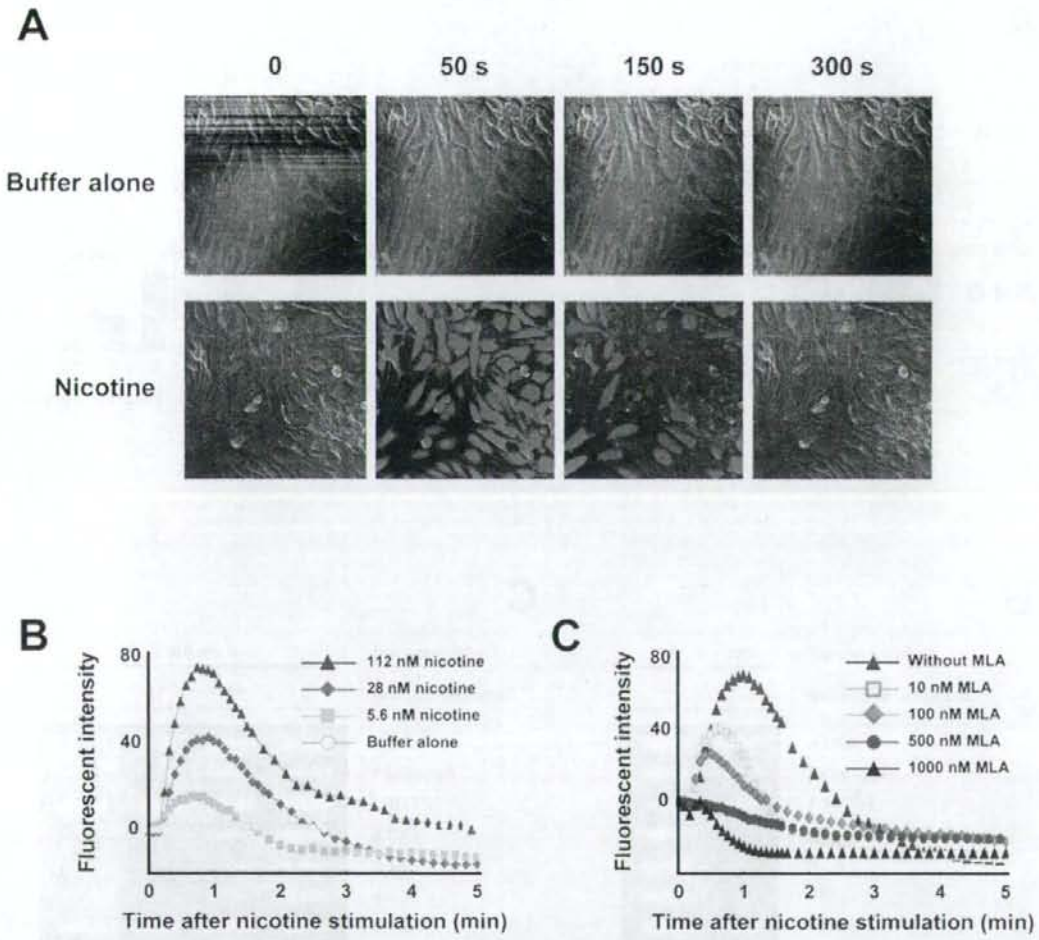

Figure 4. Calcium influx assay in primary chondrocyte culture. Nicotine-stimulated calcium signaling was investigated by the use of a fluorescent Ca^{2+} indicator. Primary chondrocyte cultures were stimulated by nicotine with or without MLA, the specific antagonist of alpha7 homomeric nAChR. A: Addition of assay buffer alone elicits no reaction (upper panels: negative control). Nicotine elicits a transient increase of intracellular calcium (lower panels). B: Nicotine elicits a transient increase of intra-cellular calcium in a concentration-dependent manner. C: MLA inhibits nicotine-induced calcium influx in a concentration-dependent manner. The cells were treated with MLA 30 min before nicotine stimulation.
doi:10.1371/journal.pone.0003945.g004

(Figure 6C). Besides, scatterplot and correlation between the FL and the BW revealed that nicotine downwardly shifted the linear slope in alpha7 nAChR +/+ fetuses but had no effect in alpha7 nAChR −/− fetuses (Figure 6D). These findings suggest that maternal nicotine exposure decreased the fetal endochondral ossification through the fetal alpha7 nAChR in vivo.

Discussion

Alpha7 nAChR was originally identified as a subunit of neuronal nAChR, and has also been shown to be functional in both neuronal and non-neuronal, i.e., non-excitable cells such as lymphocytes, vascular endothelial cells, keratinocytes and bronchial epithelium [16]. In this study, we demonstrated the expression of the alpha7 subunit of nAChR at resting to pre-hypertrophic chondrocytes in murine growth plate and on a culture of human growth plate chondrocytes, and the involvement of alpha7 nAChR in nicotine-induced delayed skeletal growth. The novel findings of alpha7 nAChR in chondrocytes suggest that the effect of smoking on delayed skeletal growth is directly correlated with nicotinic action on chondrocytes.

Direct effect of nicotine on human growth plate chondrocytes

Maternal nicotine exposure decreases the width of the hypertrophic zone of growth plate, increases apoptotic chondrocytes, and reduces the length of femur in rat [20]. Contrarily, nicotine has been shown to up-regulate glycosaminoglycan and

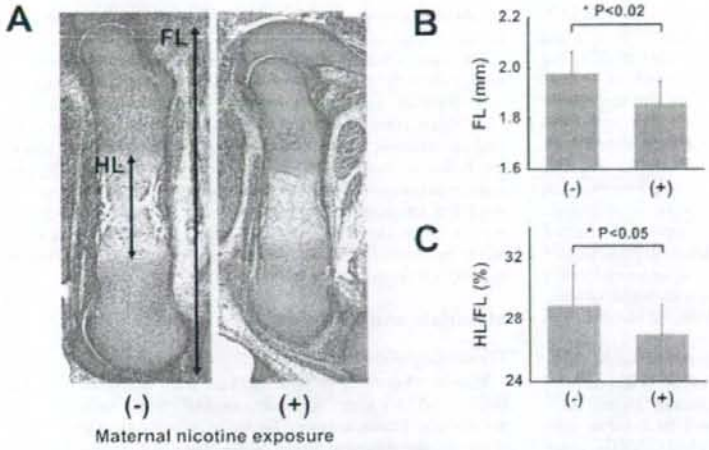

Figure 5. Maternal nicotine exposure in wild-type mice. Ovulation-induced pregnant mice were mated and were given drinking water with nicotine during pregnancy. At noon on gestational day 15, the fetuses were sacrificed, and their legs were histologically investigated. A: Skeletal growth estimated by measuring the femur length (FL) and the length of the hypertrophic zone of the femur (HL). B: FL (mm), C: HL/FL (%) of E15.5 fetuses whose mothers were given drinking water with or without nicotine. Nicotine significantly decreased FL and HL/FL.
doi:10.1371/journal.pone.0003945.g005

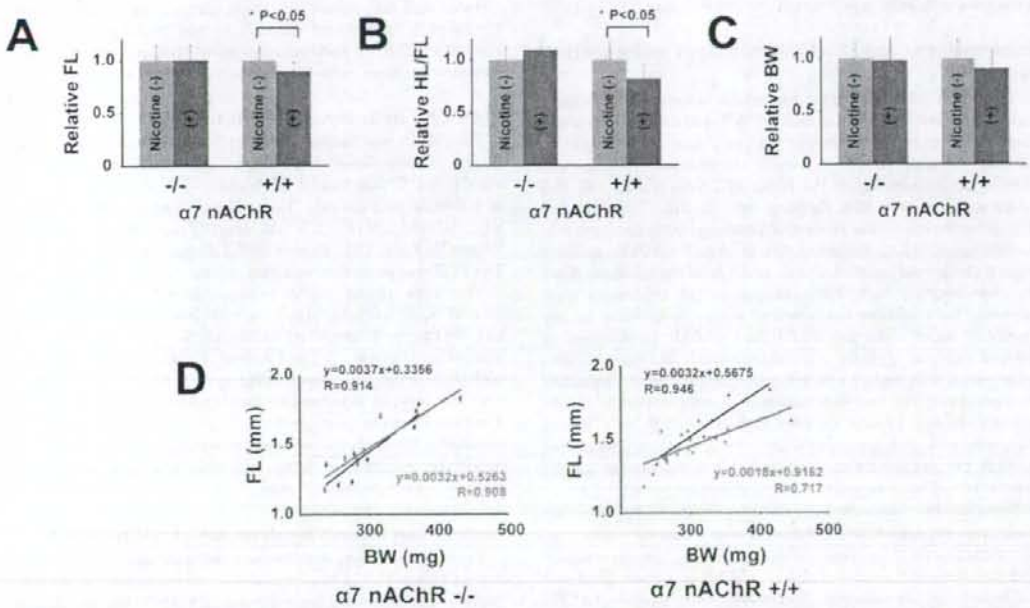

Figure 6. Maternal nicotine exposure in alpha7 nAChR-disrupted mice. A–C: FL, HL/FL, and body weight (BW) of alpha7 nAChR −/− and alpha7 nAChR +/+ E15.5 littermate fetuses. Alpha7 nAChR +/− female were mated with alpha7 nAChR +/− male, and given drinking water with or without nicotine during pregnancy. Relative FL, HL/FL, and BW were calculated, each value in mice that did not receive nicotine was regarded as equal to 1.0. Nicotine significantly reduced FL and HL/FL in alpha7 nAChR +/+ fetuses but not in alpha7 nAChR −/− fetuses (A,B). Nicotine did not significantly reduce BW in either genotype (C). D: Scatterplot and correlation between the FL and BW of mice with (red line) or without (black line) exposure to nicotine. In alpha7 nAChR +/+ fetus, Nicotine downwardly shifts the linear slope in alpha7 nAChR +/+ fetuses but not in alpha7 nAChR −/− fetuses.
doi:10.1371/journal.pone.0003945.g006

collagen synthesis of human articular chondrocytes in vitro [21]. Cultured human growth plate chondrocytes derived from infant fingers serve as a good model for analyzing whether nicotine has direct action on growth plate chondrocytes. The present findings of nicotinic effect, i.e. decreasing matrix synthesis and suppressing hypertrophic differentiation but not proliferation on growth plate chondrocytes in vitro, indicate the direct effect of nicotine on growth plate chondrocytes. The findings are consistent with reports that maternal nicotine exposure has a negative effect on endochondral ossification in animals [13]. Besides, these findings are consistent, considering the fact that longitudinal skeletal growth is partly caused by matrix synthesis and hypertrophic differentiation of chondrocytes. Confirmation of the animal model using "human" chondrocytes is essential since certain chemicals, such as thalidomide, exhibit different effects in humans and rodents.

Differences of expression levels of the genes for Col X, ALP, Ihh, MMP13, and VEGF in alginate beads culture (Figure 3B, C) may attribute to differential regulation among hypertrophic markers. Expression of the Ihh, Col X, and ALP genes were down-regulated by nicotine and the MMP13 and VEGF genes remained unaffected. Alternatively, the difference could be a result of chondrocyte culture, that is, artifactual induction ex vivo, and the MMP13 and VEGF genes were indeed expressed at the start of alginate bead culture with chondrocytes at passage 1 (Fig. 3B, lane 1: "0 W"). In contrast, the Col X, ALP, and Ihh genes were appropriately regulated after three-dimensional culture (Figure 3B, lane 2: "3 W"; Figure 3C, lane 1: without exposure to nicotine), as is the case with gene regulation in the growth plate.

Involvement of alpha7 nAChR in delayed endochondral ossification

The alpha7 nAChR-null mice exhibit normal development, including neural tissue, but alpha7 nAChR-null mice lack nicotinic currents in hippocampal neurons [22], and show abnormalities in late-stage keratinocyte development in the epidermis [23]. Lack of phenotypic abnormality in the femur of fetuses (Figure 5B) and adults indicates that ACh signaling through alpha7 nAChR has little involvement in the process of physiological skeletal growth. Results using MLA, the antagonist to alpha7 nAChR, strongly suggest the involvement of alpha7 nAChR in the nicotinic effect on chondrocytes. Such low-molecular weight substances may, however, have additional unclarified action in addition to any "specific" action. The proof of alpha7 nAChR involvement in delayed skeletal growth was strengthened by the in vivo experiments with alpha7 nAChR gene-disrupted mice. Especially so, considering the fact that maternal nicotine exposure caused delayed skeletal growth in only alpha7 nAChR +/+ fetuses compared with their alpha7 nAChR −/− littermates, fetal alpha7 nAChR but not maternal alpha7 nAChR is responsible for the mechanism of nicotine-induced delayed skeletal growth.

Since nicotine exposure has been reported to be epidemiologically and experimentally correlated with maternal effect, i.e., abnormal placental function and blood flow [10], the physiological and pathological function of alpha7 nAChR in growth plate was confirmed by comparing "littermates" of alpha7 nAChR (Figure 6B). This comparison confirms involvement of alpha7 nAChR on the fetus, and eliminates a possibility of maternal effect. Furthermore, decrease of relative femur length (Figure 6C, scatterplot and correlation, right panel, alpha7 nAChR +/+) and lack of nicotinic effect on body weight of alpha7 nAChR fetuses (Figure 6B, right panel, "BW") by maternal nicotine exposure indicate a specific effect of nicotine on bone growth rather than a systemic effect. Therefore, the effect of smoking during pregnancy on skeletal growth may be attributed to this direct action of nicotine on growth plate chondrocytes, at least in part.

Our studies suggest that, from the large number of chemicals associated with cigarette smoking, nicotine may cause delayed skeletal growth and, indeed, amniotic fluid and breast milk both have higher concentrations of nicotine than maternal serum does [24]. In addition, metabolism of nicotine in the fetus and child is much slower than that in adults [25]. We therefore should pay close attention to the effect of smoking, regardless of being active or passive, on growth plate chondrocytes. This nicotinic effect may also extend to the delay of fracture repair or generation of non-union in adults, since the process of bone repair also partly depends on endochondral ossification.

Materials and Methods

Chondrocyte cultures

Human chondrocytes were isolated from epiphysis of extra fingers, which were surgically excised from patients with polydactyly. Ethical approval for tissue collection was granted by the Institutional Review Board of the National Research Institute for Child Health and Development, Tokyo, Japan (#88). Minced tissue was incubated for 1 h at 37°C in 0.08% trypsin in PBS, then for 6 h at 37°C in 0.2% collagenase type 1 (Wako, Osaka, Japan) in Dulbecco's Modified Eagle's medium (DMEM). The released cells were washed and resuspended in DMEM containing 10% fetal bovine serum (FBS, Sanko Junyaku Co., Tokyo, Japan, lot number: 27110307) and plated at a density of 1×10^6 cells per 100 mm dish for primary monolayer cultures, or 1×10^6 cells per 35 mm dish for calcium influx assay and immunocytochemical assay of nAChR. In each experiment, we used one lot of cultured chondrocytes from extra fingers obtained from four patients.

RT-PCR for detection of nAChR subunit

Total RNA was prepared from epiphysis of extra fingers using Isogen (Nippon Gene) according to the manufacturer's recommendations. DNase-treated RNA was reverse transcribed in 20 µl of RT-PCR mix (50 mM Tris, pH 8.3, 3 mM $MgCl_2$, 75 mM KCl, 50 mM dNTPs, 2.5 µM oligo$(dT)_{20}$, 5 mM DTT, 2 U RNaseOUT and 10 U SuperScriptIII (Invitrogen) at 50°C for 1 h. The PCR was performed in a final volume of 50 µl containing 1 µl of the single strand cDNA product, 25 mM TAPS (pH 9.3), 50 mM KCl, 2.0 mM $MgCl_2$, 1 mM β-mercaptoethanol , 200 µM dNTPs, and AmpliTaq Gold (Applied Biosystems) and 20 pmol of each forward (5′) and reverse (3′) primers (Table S1). For each experiment the housekeeping gene GAPDH was amplified with 25–35 cycles to normalize the cDNA content of the samples. The amplification was performed for 30 cycles, with other conditions following polymerase-producing manufacturer's recommendations. Human brain and skeletal muscle RNAs were purchased from Ambion (Austin, TX).

Western blot analysis for detection of nAChR subunit

Total proteins were isolated from primary monolayer cultures using CelLyticTM-M Mammalian Cell Lysis/Extraction Reagent (Sigma). The proteins were separated by SDS-PAGE (Bio-Rad) in a 10% acrylamide gel, then blotted at 60 V for 2 h at 4°C onto a nitrocellulose membrane. Non-specific binding was blocked by incubation in TBS containing 10% BSA and 0.05% Tween-20. The membrane was subsequently incubated at 4°C overnight with the monoclonal antibody to nicotinic acetylcholine receptor, alpha7 subunit (Sigma, St-Louis, MO; product number: N 8158) diluted 1:3000. After rinsing, the membrane was incubated for 1 h at room temperature in horseradish peroxidase-conjugated rabbit

anti-rat IgG antibody (Sigma; A 5795) at a dilution of 1:3000 in TBS containing 0.05% Tween-20. After rinsing, the membrane was immersed in ECL solution (GE Healthcare, Buckinghamshire, UK). Then, the blots were visualized by LAS-1000plus IDX2, the luminescent image analyzer (Fuji Photo Film, Japan).

Immunocytochemical and immunohistochemical analysis

Immunocytochemical analysis was performed as previously described [26]. Briefly, dishes were incubated with antibody to alpha7 subunit of nAChR in PBS containing 1% BSA. As a methodological control, the primary antibody was omitted. After washing in PBS, dishes were incubated with horseradish peroxidase (HRP)-conjugated rabbit anti-rat IgG antibody. Staining was developed by using a solution containing diaminobenzidine and 0.01% H_2O_2 in 0.05 M Tris-HCl buffer, pH 6.7.

For immunohistochemical analysis, hind legs of E15.5 C57BL/6J mice were prepared, fixed in 4% paraformaldehyde phosphate buffer solution (Wako) overnight at 4°C, and embedded in paraffin. Immunohistochemical analysis was performed as previously described [27]. Briefly, slides were treated with 0.4% pepsin (DAKO) at 37°C for 30 min, incubated with primary antibody to alpha7 subunit of nAChR(Sigma, product number: N 8158) diluted 1:2000 in PBS containing 1% BSA at room temperature for 3 h, and incubated with simple mouse stain MAX-PO (RAT), a second antibody, at room temperature for 1 h. Staining was developed by using a solution containing diaminobenzidine and 0.01% H_2O_2 in 0.05 M Tris-HCl buffer, pH 6.7. Finally, slides were counterstained with hematoxylin.

Agarose gel cultures

Chondrocytes were cultured in agarose-stabilized suspension using a modified method as previously described [28]. Primary monolayer cultures were trypsinized, re-suspended in agarose gel medium : DMEM/F-12 containing 10% FBS, 100 units/ml penicillin G, 100 mg/ml streptomycin, and 50 mg/ml ascorbate, to a concentration of 2×10^4 cells/ml, then mixed with equal volume of 1% low-temperature melting agarose (Sigma-Aldrich, Steinheim, Germany) in agarose gel medium, giving a final concentration of 1×10^4 cells/ml suspended in 0.5% low-temperature melting agarose in agarose gel medium (suspension agarose). Three milliliters of suspension agarose were added to 60 mm culture plates that were precoated with 2 ml of 1% autoclaved standard agarose (Bio-Rad, Hercules, CA). The gel was allowed to solidify at 4°C before addition of agarose gel medium. Then, culture plates were placed in a 37°C, 5% CO_2 humidified incubator for 21 days, and medium containing indicated concentration of nicotine was replaced once at the beginning of the week. After 21 days, suspension agarose was transferred to a glass slide, and placed on a plate warmer at 50°C with a covering of positively-charged nylon membranes (Roche, Mannheim, Germany). The slides were completely dried in a incubator at 42°C overnight, and fixed in 4% paraformaldehyde for 15 min, and stained with ALB to identify colonies producing glycosaminoglycans and to observe histologically. Colonies were defined as a cluster of cells with a diameter greater than 50 μm. ALP activity was determined in non-fixed agarose slide by Histofine, ALP substrate kit (Nichirei, Tokyo, Japan) following the manufacturer's product information. Type 10 collagen expression was also determined in the agarose slide using specific monoclonal antibody (Sigma; product number: C7974). The slide was fixed in acetone (Nacalai Tesque, Kyoto, Japan) at room temperature for 20 min. Non-specific binding was blocked with 2.5% normal rabbit serum (DakoCytomation, Glostrup, Denmark) in PBS containing 1% BSA and 1% Triton X-100. Slides were incubated for 6 h at room temperature with primary antibody, diluted 1:2000 in PBS containing 1% BSA. Bound antibody was detected by HRP-conjugated polyclonal rabbit anti-mouse IgM antibody (Dako, Glostrup, Denmark; product number: P 0260) diluted 1:100 in PBS at room temperature for 30 min. Peroxidase activity was visualized with diaminobenzidine tetrahidrochloride plus 0.03% H_2O_2, and slide was counterstained with hematoxylin.

Alginate bead cultures

Chondrocytes were cultured in alginate beads following the method described by De Ceuninck et al. Primary monolayer cultures were trypsinized, washed, and centrifuged. The isolated chondrocytes were suspended at a concentration of 2×10^6 cells/ml in a 1.25% alginate in 0.15 M NaCl. The cell suspension was slowly expressed through a 21 gauge needle and dropped into a 102 mM $CaCl_2$ solution. The beads with approximately 25,000 cells/bead were allowed to polymerize for 10 min and washed three times with 0.15 M NaCl, followed by two washes in DMEM/F12. The beads were then transferred to medium (200 beads/10 ml/60 mm culture dish): DMEM/F-12 containing 10% FBS, 50 μg/ml ascorbate, 100 units/ml penicillin G, 100 mg/ml streptomycin. The beads were cultured at 37°C in a 5% CO_2 humidified incubator for four months, and medium with or without nicotine was replaced twice weekly. The beads were transferred to new dishes every other week to avoid the formation of monolayer cultures on the bottom of the dish by chondrocytes escaping from the beads.

For histological analysis, the beads were fixed in 4% paraformaldehyde, 0.1 M cacodylate buffer, pH 7.4, containing 10 mM $CaCl_2$ for 4 h at room temperature, and then washed overnight at 4°C in 0.1 M cacodylate buffer, pH 7.4, containing 50 mM $BaCl_2$. The beads were dehydrated through alcohols and embedded in paraffin. The sections were routinely stained with ALB and safranin-O.

For RT-PCR analysis, chondrocytes were separated from the beads by incubating the beads in dissolution solution (at a ratio of 200 μl/bead), containing 55 mM EDTA, for 5 min and centrifuged. Total RNA was isolated by using RNeasy (Qiagen) following manufacturer's instructions, and was converted to cDNA by same method as described above. The sequences of PCR primers of human chondrocyte-related gene are listed in Table S2. PCR was performed in a final volume of 50 μl containing 2 μl of the single strand cDNA product (10 ng/μl), 10 mM Tris-HCl (pH8.3), 50 mM KCl, 1.5 mM $MgCl_2$, 200 μM dNTPs, 1.25 U Taq (Takara), and 20 pmol of each forward (5′) and reverse (3′) primers.

Calcium imaging

Primary monolayer cultures in 35 mm glass-bottomed plates were prepared. At near confluence, measurement was done by using Fluo-4 NW calcium assay kit (Molecular Probes, product number: F36206) following the manufacturer's product information. In short, the cells were incubated in dye loading solution containing 2.5 mM probenecid at 37°C for 30 min, then at room temperature for an additional 30 min before nicotine stimulation. The fluorescence was measured in LSM 510 (Carl Zeiss) with the settings appropriate for argon laser. Nicotine and its antagonists were prepared as a solution in assay buffer. If antagonists were used, they were added 30 min prior to nicotine stimulation.

Maternal nicotine exposure in wild-type mice

Three-month-old pregnant mice were purchased at day 1 of pregnancy from Sankyo Laboratories (Tokyo, Japan). The mice were given drinking water containing 2% sucrose (Wako, Osaka, Japan) with or without nicotine (hydrogen tartrate salt; Sigma-

Aldrich, St. Louis, MO). Nicotine was added to the sucrose solution starting at an initial concentration of 25 μg/ml to the treatment group mice. This was increased to 50 μg/ml on days 3 to 4, 100 μg/ml after day 5. The control mice were given only sucrose solution as a drinking water. The pregnant mice were sacrificed at noon on gestational day 15. The embryo were immediately weighed, and the legs were immediately removed and fixed in 4% paraformaldehyde phosphate buffer solution (Wako) for 24 h. Then, the legs were dehydrated through alcohols, embedded in paraffin, and sections were stained with Hematoxylin and Eosin for histological analysis.

Maternal nicotine exposure in alpha7 nAChR-disrupted mice

B6.129S7-Chrna7<tm1Bay>/J, the alpha7 nAChR +/− mice were obtained from Charles River Laboratories Japan. Ten- to 12-week old alpha7 nAChR +/− mice were mated, and pregnant mice were given sucrose solution with or without nicotine. The fetuses were obtained and analyzed as in the case of wild-type C57BL/6J mice, as described above. The alpha7 nAChR genotype was determined by means of PCR reaction with the specific primers (Table S3).

Statistics

The results of the quantative assays were expressed as mean±S.D. Significance was determined with Student's *t* test and ANOVA. All experiments were replicated twice.

Supporting Information

Figure S1 In vivo chondrocytic proliferation assay. A: Paraffin section of the femur of E15.5 C57BL/6J mice immunohistochemically stained with antibody to PCNA. Proliferative chondrocytes extensively stained positive for PCNA regardless of maternal nicotine exposure. B: Percentage of PCNA-positive cells in chondrocytes of the proliferative zone. There is no significant difference between the two groups. Hind legs of E15.5 C57BL/6J mice were prepared, fixed in 4% paraformaldehyde phosphate buffer solution (Wako) overnight at 4°C, and embedded in paraffin. After deparaffinization, slides were autoclaved in 0.01 M citrate buffer (pH 6.0) for 10 min, incubated with primary antibody to PCNA (DAKO: PC10) diluted 1:400 in PBS containing 1% BSA at room temperature for 3 h, and incubated with polyclonal rabbit anti-mouse immunoglobrins/HRP (DAKO: P260) at room temperature for 1 h. Staining was undertaken using a solution containing diaminobenzidine and 0.01% H_2O_2 in 0.05 M Tris-HCl buffer at pH 6.7, followed by counterstaining with hematoxylin.
Found at: doi:10.1371/journal.pone.0003945.s001 (0.06 MB PDF)

Table S1 Primers for nAChR subunit genes
Found at: doi:10.1371/journal.pone.0003945.s002 (0.03 MB PDF)

Table S2 Primers for chondrocyte specific genes
Found at: doi:10.1371/journal.pone.0003945.s003 (0.01 MB PDF)

Table S3 Primers for genotypying alpha7 nAChR gene
Found at: doi:10.1371/journal.pone.0003945.s004 (0.01 MB PDF)

Acknowledgments

We would like to express our sincere thanks to M. Nasu, C-H. Cui, H. Akutsu, K. Miyado, and M. Toyoda for support throughout this work, to H. Abe for providing expert technical assistance, to K. Saito and Y. Ito for their secretarial work, and to A. Crump for reviewing the manuscript.

Author Contributions

Conceived and designed the experiments: AK AU. Performed the experiments: AK HM. Analyzed the data: AK HM AU. Contributed reagents/materials/analysis tools: KS HI ST YT. Wrote the paper: AK AU.

References

1. Davies DP, Abernethy M (1976) Cigarette smoking in pregnancy: Associations with maternal weight gain and fetal growth. Lancet 1: 385–387.
2. Hardy JB, Mellits ED (1972) Does maternal smoking during pregnancy have a long-term effect on the child? Lancet 2: 1332–1336.
3. Wingerd J, Schoen EJ (1974) Factors influencing length at birth and height at five years. Pediatrics 53: 737–741.
4. Karatza AA, Varvarigou A, Beratis NG (2003) Growth up to 2 years in relationship to maternal smoking during pregnancy. Clin Pediatr (Phila) 42: 533–541.
5. Sexton M, Hebel JR (1984) A clinical trial of change in maternal smoking and its effect on birth weight. Jama 251: 911–915.
6. Yerushalmy J (1971) The relationship of parents' cigarette smoking to outcome of pregnancy–implications as to the problem of inferring causation from observed associations. Am J Epidemiol 93: 443–456.
7. Olsen J, Pereira Ada C, Olsen SF (1991) Does maternal tobacco smoking modify the effect of alcohol on fetal growth? Am J Public Health 81: 69–73.
8. Trygg K, Lund-Larsen K, Sandstad B, Hoffman HJ, Jacobsen G, et al. (1995) Do pregnant smokers eat differently from pregnant non-smokers? Paediatr Perinat Epidemiol 9: 307–319.
9. Haddon W Jr, Nesbitt RE, Garcia R (1961) Smoking and pregnancy: carbon monoxide in blood during gestation and at term. Obstet Gynecol 18: 262–267.
10. Mochizuki M, Maruo T, Masuko K (1985) Mechanism of foetal growth retardation caused by smoking during pregnancy. Acta Physiol Hung 65: 295–304.
11. Nordstrom ML, Cnattingius S (1996) Effects on birthweights of maternal education, socio-economic status, and work-related characteristics. Scand J Soc Med 24: 55–61.
12. Mau G (1976) Letter: Smoking and the fetus. Lancet 1: 972.
13. Nelson E, Jodscheit K, Guo Y (1999) Maternal passive smoking during pregnancy and fetal developmental toxicity. Part 1: gross morphological effects. Hum Exp Toxicol 18: 252–256.
14. El-Zawawy HB, Gill CS, Wright RW, Sandell LJ (2006) Smoking delays chondrogenesis in a mouse model of closed tibial fracture healing. J Orthop Res 24: 2150–2158.
15. Olsen J (1992) Cigarette smoking in pregnancy and fetal growth. Does the type of tobacco play a role? Int J Epidemiol 21: 279–284.
16. Sharma G, Vijayaraghavan S (2002) Nicotinic receptor signaling in nonexcitable cells. J Neurobiol 53: 524–534.
17. Arneric SP, Brioni JD (1999) Neuronal nicotinic receptors : pharmacology and therapeutic opportunities. New York: Wiley-Liss, xii, 421 p.
18. Tacchetti C, Quarto R, Nitsch L, Hartmann DJ, Cancedda R (1987) In vitro morphogenesis of chick embryo hypertrophic cartilage. J Cell Biol 105: 999–1006.
19. Hauselmann HJ, Fernandes RJ, Mok SS, Schmid TM, Block JA, et al. (1994) Phenotypic stability of bovine articular chondrocytes after long-term culture in alginate beads. J Cell Sci 107 (Pt1): 17–27.
20. Kurtoglu S, Gunes T, Koklu E, Bastug O, Canoz O, et al. (2007) Influence of maternal nicotine exposure on neonatal rat bone: protective effect of pentoxifylline. Exp Biol Med (Maywood) 232: 398–405.
21. Gullahorn L, Lippiello L, Karpman R (2005) Smoking and osteoarthritis: differential effect of nicotine on human chondrocyte glycosaminoglycan and collagen synthesis. Osteoarthritis Cartilage 13: 942–943.
22. Orr-Urtreger A, Goldner FM, Saeki M, Lorenzo I, Goldberg L, et al. (1997) Mice deficient in the alpha7 neuronal nicotinic acetylcholine receptor lack alpha-bungarotoxin binding sites and hippocampal fast nicotinic currents. J Neurosci 17: 9165–9171.
23. Arredondo J, Nguyen VT, Chernyavsky AI, Bercovich D, Orr-Urtreger A, et al. (2002) Central role of alpha7 nicotinic receptor in differentiation of the stratified squamous epithelium. J Cell Biol 159: 325–336.
24. Luck W, Nau H, Hansen R, Steldinger R (1985) Extent of nicotine and cotinine transfer to the human fetus, placenta and amniotic fluid of smoking mothers. Dev Pharmacol Ther 8: 384–395.

25. Dempsey D, Jacob P 3rd, Benowitz NL (2000) Nicotine metabolism and elimination kinetics in newborns. Clin Pharmacol Ther 67: 458–465.
26. Sano M, Umezawa A, Abe H, Akatsuka A, Nomaka S, et al. (2001) EAT/mcl-1 expression in the human embryonal carcinoma cells undergoing differentiation or apoptosis. Exp Cell Res 266: 114–125.
27. Sano M, Umezawa A, Suzuki A, Shimoda K, Fukuma M, et al. (2000) Involvement of EAT/mcl-1, an anti-apoptotic bcl-2-related gene, in murine embryogenesis and human development. Exp Cell Res 259: 127–139.
28. Benya PD, Shaffer JD (1982) Dedifferentiated chondrocytes reexpress the differentiated collagen phenotype when cultured in agarose gels. Cell 30: 215–224.

Human Sclera Maintains Common Characteristics with Cartilage throughout Evolution

Yuko Seko[1,2], Noriyuki Azuma[2], Yoriko Takahashi[1], Hatsune Makino[1], Toshiyuki Morito[3], Takeshi Muneta[3], Kenji Matsumoto[4], Hirohisa Saito[4], Ichiro Sekiya[5], Akihiro Umezawa[1]*

1 Department of Reproductive Biology and Pathology, National Institute for Child and Health Development, Tokyo, Japan, 2 Department of Ophthalmology, National Center for Child Health and Development, Tokyo, Japan, 3 Section of Orthopaedic Surgery, Tokyo Medical and Dental University, Tokyo, Japan, 4 Department of Allergy and Immunology, National Institute for Child and Health Development, Tokyo, Japan, 5 Section of Cartilage Regeneration, Tokyo Medical and Dental University, Tokyo, Japan

Abstract

Background: The sclera maintains and protects the eye ball, which receives visual inputs. Although the sclera does not contribute significantly to visual perception, scleral diseases such as refractory scleritis, scleral perforation and pathological myopia are considered incurable or difficult to cure. The aim of this study is to identify characteristics of the human sclera as one of the connective tissues derived from the neural crest and mesoderm.

Methodology/Principal Findings: We have demonstrated microarray data of cultured human infant scleral cells. Hierarchical clustering was performed to group scleral cells and other mesenchymal cells into subcategories. Hierarchical clustering analysis showed similarity between scleral cells and auricular cartilage-derived cells. Cultured micromasses of scleral cells exposed to TGF-βs and BMP2 produced an abundant matrix. The expression of cartilage-associated genes, such as Indian hedge hog, type X collagen, and MMP13, was up-regulated within 3 weeks in vitro. These results suggest that human 'sclera'-derived cells can be considered chondrocytes when cultured ex vivo.

Conclusions/Significance: Our present study shows a chondrogenic potential of human sclera. Interestingly, the sclera of certain vertebrates, such as birds and fish, is composed of hyaline cartilage. Although the human sclera is not a cartilaginous tissue, the human sclera maintains chondrogenic potential throughout evolution. In addition, our findings directly explain an enigma that the sclera and the joint cartilage are common targets of inflammatory cells in rheumatic arthritis. The present global gene expression database will contribute to the clarification of the pathogenesis of developmental diseases such as high myopia.

Citation: Seko Y, Azuma N, Takahashi Y, Makino H, Morito T, et al. (2008) Human Sclera Maintains Common Characteristics with Cartilage throughout Evolution. PLoS ONE 3(11): e3709. doi:10.1371/journal.pone.0003709

Editor: Che John Connon, University of Reading, United Kingdom

Received July 31, 2008; **Accepted** October 8, 2008; **Published** November 12, 2008

Funding: This study was supported by Research Fellowships of the Japan Society for the Promotion of Science (JSPS) for Young Scientists; a grant from the Ministry of Education, Culture, Sports, Science and Technology (MEXT) of Japan and Health and Labor Sciences Research Grants; by a Research grant on Health Science Focusing on Drug Innovation from the Japan Health Science Foundation; by the Program for Promotion of Fundamental Studies in Health Science of the Pharmaceuticals and Medical Devices Agency; by a grant from the Terumo Life Science Foundation; by a Research Grant for Cardiovascular Disease from the Ministry of Health, Labor and Welfare; and by a Grant for Child Health and Development from the Ministry of Health, Labor and Welfare.

Competing Interests: The authors have declared that no competing interests exist.

* E-mail: umezawa@1985.jukuin.keio.ac.jp

Introduction

The eye receives information from the outside as the retinal image, converting it into electrical signals for the brain, leading to visual perception. The retinal image is stabilized by the balance of intraocular pressure and the curvatures of the scleral and corneal envelope. In order to keep this balance, the rigidity of the sclera and the cornea are essential, especially the sclera must be rigid enough for the eyeball to be rotated by powerful extraocular muscles adhering to the sclera. The sclera and the corneal stroma that are anatomically continuous have common characteristics such as mechanical rigidity, and share a common origin, i.e., the neural crest. However, the cornea and the sclera are different in transparency: the cornea is completely transparent to produce a sharp image on the retina; the sclera is opaque to avoid the internal light scattering affecting the retinal image. This corneal transparency has been attributed to significant changes in the structure, especially of collagen fibrils, in the latter stages of development [1]. Multipotent progenitor/precursor cells of corneal stroma are identified from the mouse eye [2]. On the other hand, existence of multipotent progenitor/precursor cells in the sclera remains unclarified. Although the sclera does not contribute significantly to visual perception, scleral diseases such as refractory scleritis, scleral perforation and pathological myopia are considered incurable or difficult to cure.

Microarray analysis of murine scleral development [3] and global sequencing analysis from the human scleral cDNA library [4] have been reported. To clarify pathogenesis of developmental diseases such as high myopia, a database of genes expressed in the sclera of younger donors is important. We here demonstrate with a global expression database of human infant sclera that the sclera derived from the neural crest evolutionarily retains characteristics of cartilage.

Results

Isolation and cell culture of human scleral cells

Scleral tissues were excised from surgical specimens collected during treatment for retinoblastoma. The scleral tissue was cut into smaller pieces and cultured in the growth medium. The scleral cells began growing out almost one week after the start of cultivation. Scleral cells exhibited a fibroblast-like spindle shape or polygonal shape in morphology when cultured in monolayer (Fig. 1A). The cells from PD 5 to PD 31 rapidly proliferated in culture, and propagated continuously (Fig. 1B). The cells stopped replicating and became broad and flat at PD 43 or 264 days, indicating that they had entered senescence. The morphological changes are PD-dependent.

Global outlook by hierarchical clustering and PCA

To clarify the specific gene expression profile of scleral cells, we compared the expression levels of 54,675 probes in the cultured scleral cells and other cultured cells (Table 1) using the Affymetrix GeneChip oligonucleotide arrays. We first performed hierarchical clustering and PCA on the expression pattern. PCA showed similarity between scleral cells and chondrocytes derived from elastic cartilage (Fig. 2A). Hierarchical clustering analysis based on all probes showed similarity between scleral cells and chondrocytes (Fig. 2B). This similarity led us to hypothesize that the scleral cells are chondrocytes when proliferated ex vivo, or have a chondrogenic potential. We then performed PCA from the expression data of cartilage-associated genes, including aggrecan, Sox9, and parathyroid hormone receptor (Table S1). These genes are categorized as "cartilage condensation" or "proteoglycan biosynthesis" according to Gene Ontology. PCA based on cartilage-associated genes demonstrated that scleral cells are grouped into the same category that includes chondrocytes, synovial cells, and synovial fluid-derived cells (Fig. 2C). The synovial cells and synovial fluid-derived cells used in this study have a strong chondrogenic potential [5–7]. Hierarchical clustering analysis based on the cartilage-associated genes also demonstrated that sclera, cartilage, synovium, and joint fluid are categorized into the same group (Fig. 2D, Fig. 2E, Fig. S1).

Table 1. Human cells analyzed in this study.

Title	Description
Bone marrow	Bone marrow-derived cell (P1)
Hepatocyte	Hepatocyte (P0)
Endometrium	Endometrial cell
Synovium	Synovium-derived cell (P1)
Joint fluid	Joint fluid-derived cell (P1)
Muscle	Muscle-derived cell (P1)
Bone	Cancellous bone-derived cell (P1)
Fat	Subcutaneus fat-derived cell (P1)
Amniotic epithelium	Amniotic epithelial cell (P4)
Umbilical cord (1)	Umbilical cord-derived cell (P0) (1)
Umbilical cord (2)	Umbilical cord-derived cell (P0) (2)
Cartilage	Auricular cartilage-derived cell (P1)
Sclera	Sclera-derived cell (P1)
Cornea (stroma)	Keratocyte (P1)
Periostium	Periostium-derived cell (P1)
Dermis	Dermal fibroblast (P2)
Cortical bone	Cortical bone-derived cell (P3)

Gene chip analysis was performed using RNAs from the cells obtained from each tissue. The cells obtained from bone marrow, liver, synovium, joint fluid, muscle, bone, and fat were cultivated as previously described [31–33]. Amniotic epithelial cells and umbilical cord-derived cells were cultured after each tissue was manually separated from the placenta and minced by surgical knife and scissors. Auricular cartilage-derived cells, periostium-derived cells, dermal fibroblasts, and cortical bone-derived cells started to be cultured after each tissue was manually separated from surgical specimens from patients with polydactyly or microtia. Keratocytes and scleral cells were obtained from corneal stroma and sclera (also see the Materials and Methods section). "Endometrium" was obtained from the homogenized endometrial cells under liquid nitrogen. All cells were harvested under signed informed consent, with the approval of the Ethics Committee of the National Institute for Child and Health Development, Tokyo. Signed informed consent was obtained from donors and the surgical specimens were irreversibly de-identified. All experiments handling human cells and tissues were performed in line with the Tenets of the Declaration of Helsinki. Global gene expression profiles of those cells are uploaded to GEO accession #:GSE10934 at http://www.ncbi.nlm.nih.gov/geo/index.cgi.

P: passage. P0 and P1 represents primary cell culture and cell culture one passage after starting primary culture from tissues, respectively.

doi:10.1371/journal.pone.0003709.t001

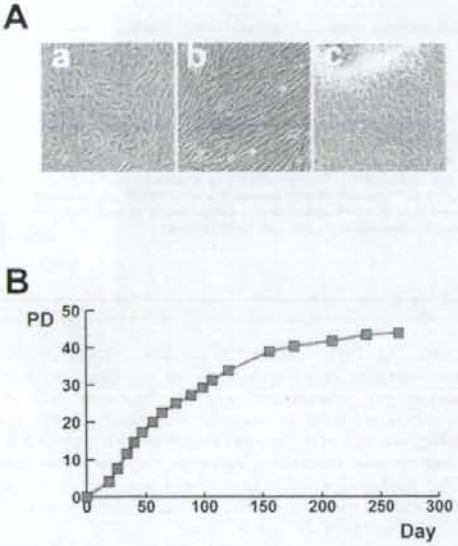

Figure 1. Proliferation of human 'sclera'-derived cells. A. Photograph of primary cultured human 'sclera'-derived cells by phase-contrast microscope. **B.** Growth curve of cultured human 'sclera'-derived cells. Vertical axis indicates population doublings (PD) and horizontal axis indicates days after innoculation of human 'sclera'-derived cells.

doi:10.1371/journal.pone.0003709.g001

Chondrogenesis of human scleral cells

After reaching 70–80% sub-confluence, we started the micromass culture of scleral cells. Four weeks after culture in a chondrogenic medium containg TGF-β1 and BMP2, a pellet of human scleral cells exhibited a spherical shape (Fig. 3A). This pellet showed an alcian blue positive extracellular matrix, indicating that cultured micromasses of scleral cells exposed to TGF-β1 and BMP2 produce an abundant matrix (Fig. 3B). RT-PCR analysis demonstrated that scleral cells at passage 0 expressed aggrecan, COL2A, SOX5, SOX6, SOX9, and PTHR1 mRNAs

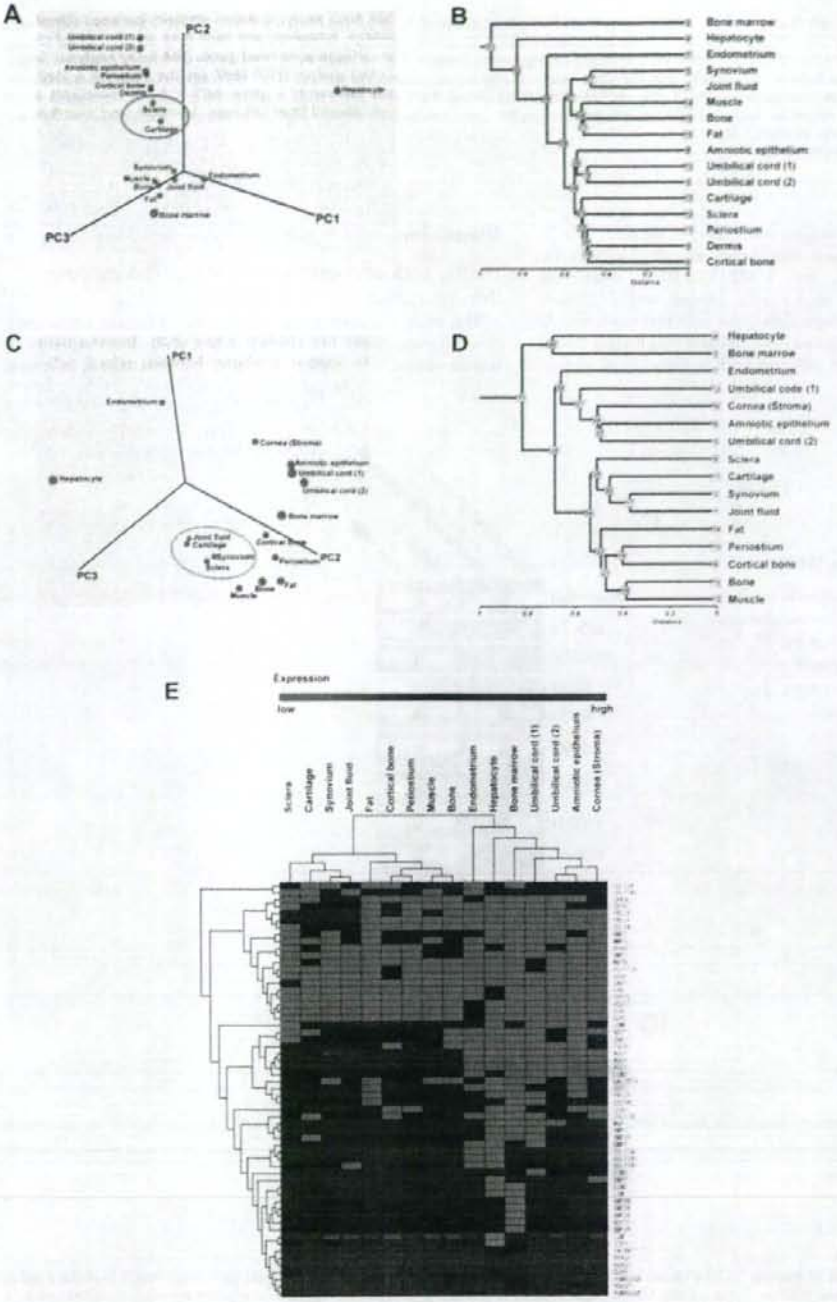

Figure 2. Global gene expression analysis of cultured human cells. A. Three-dimensional representation of PCA of gene expression levels (Human Genome U133 Plus 2.0: 54,675 probes). The gene expression data from scleral cells following one passage from the primary cultured cells (equivalent to appropriately 4 PDs) were used for PCA. Sclera and cartilage are positioned closely adjacent (shown in circle). **B.** Hierarchical clustering

analysis based on the expression of all genes (Human Genome U133 Plus 2.0: 54,675 probes, NIA Array Analysis) shows similarity between scleral cells and chondrocytes. **C**. PCA of the cartilage-associated gene expression (Table S1). Sclera, cartilage, synovium, and joint fluid are positioned closely adjacent (shown in circle). **D**. Hierarchical clustering analysis based on expression levels of the cartilage-associated genes (NIA Array Analysis). Sclera, cartilage, synovium, and joint fluid are categorized into the same group. **E**. Hierarchical clustering analysis (TIGR MeV, see the Materials & Methods) with the heat map, based on expression levels of the cartilage-associated genes. Each row represents a gene; each column represents a cell population. Sclera, cartilage, synovium, and joint fluid are categorized into the same group. Cells derived from cartilage, synovium, and joint fluid are capable of generating cartilage in vivo [7,34].
doi:10.1371/journal.pone.0003709.g002

(Fig. 3C). These expressions were maintained in the cells after 10 population doublings. After in vitro chondrogenesis of scleral cells, COL10A, SOX5, IHH, and MMP13 mRNA expressions increased. After human scleral cells labeled with DiI were implanted into a rat cartilage defect, the cells expressed type II collagen (Fig. 3D). These results demonstrated that human scleral cells retained chondrogenic potential both in vitro and in vivo.

Discussion

Tracing back of human scleral cells to chondrocytes through cultivation

This study was undertaken to investigate if human sclera has a chondrogenic nature like chicken sclera [8,9]. Bioinformatics of human scleral cells suggest similarity between scleral cells and

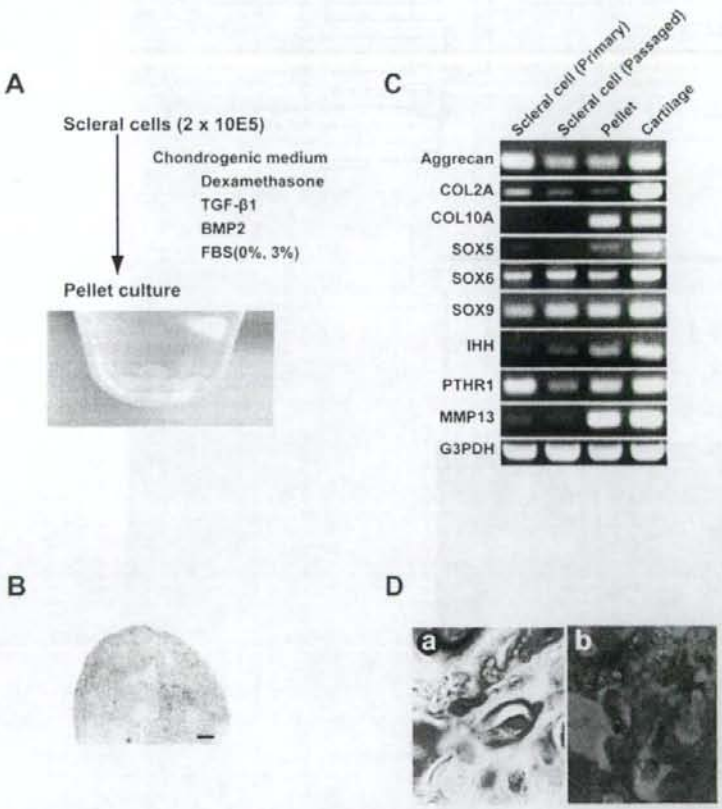

Figure 3. Chondrogenesis of human 'sclera'-derived cells. A. In vitro chondrogenesis. 'Sclera'-derived cells were centrifuged to make a pellet and cultured in chondrogenic medium for 4 weeks. Macroscopic feature is shown. **B**. Histological section of a pellet by micromass culture in a chondrogenic medium stained with alcian blue. Bar: 100 μm. **C**. Reverse transcriptase-PCR for cartilage-associated genes. Total RNAs were prepared from scleral cells at passage 0, at 10 population doublings, after in vitro chondrogenic induction, and normal cartilage as a positive control. **D**. Histological sections 4 weeks after transplantation of human scleral cells into cartilage defect of the knee in a rat. (a) Toluidin blue staining. (b) Immunohistochemistry. Human scleral cells were labeled with DiI (red). Nuclei were stained with DAPI (blue). Type II collagen was shown as green.
doi:10.1371/journal.pone.0003709.g003

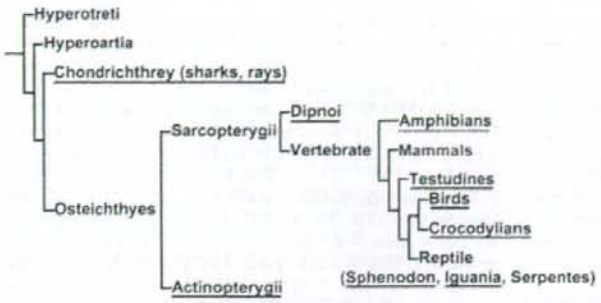

Figure 4

Figure 4. The distribution of scleral cartilage in vertebrates. The chondrogenic nature of the sclera is conserved across species. The figure is modified from Franz-Odendaal, TA, et al., 2006 [10]. Species that have cartilage in the sclera are underlined; species with either absence or presence of cartilage in the sclera, depending on family, are dot-underlined; species without cartilage in the sclera are non-underlined.
doi:10.1371/journal.pone.0003709.g004

chondrocytes, and this similarity may be attributed to evolution of the sclera (Fig. 4), that is, animals such as elasmobranch, teleost fish, amphibians, reptiles and birds incorporate the development of a cup of hyaline cartilage in the sclera [10]. Scleral cartilage is hypothesized to counter against the traction force of the extraocular muscle and against the accommodative force to move or deform the lens by intraocular muscles. In this paper, we employ the global gene expression approach to human scleral cells. As a result, scleral cells and chondrocytes are found to share common chondrogenic characteristics.

Simulation of chondrogenic process during development

The phenotype of the differentiated chondrocyte is characterized by the synthesis, deposition, and maintenance of cartilage-specific extracellular matrix molecules, including type II collagen and aggrecan [11–13]. Three-dimensional culture is a prerequisite for exhibition of this chondrogenic phenotype in vitro since the phenotype of differentiated chondrocytes is unstable in culture and is rapidly lost during serial monolayer subculturing [14–16]. The expression pattern of cartilage-associated genes in sclera-derived cells after induction is consistent with that of chondrocytes during development (Fig. 3C, Fig. S2): a) Consistent expression of type II collagen and aggrecan, markers of early-phase chondrogenesis [17,18] in sclera-derived cells, indicates that sclera-derived cells retain their chondrogenic nature as a default state; b) Induction of type X collagen and MMP13 genes after pellet formation of sclera-derived cells may simulate late-stage chondrogenesis. In addition, other chondrocyte-associated genes, such as sox5, IHH, and PTHR1 were also up-regulated. Sox5 functions as a transcription factor necessary for chondrogenesis [19,20], IHH promotes chondrogenesis as a cytokine [21], and PTHR1 mediates parathyroid hormone signaling as a specific receptor [18]. These results suggest that ex vivo culture of sclera-derived cells simulates the developmental process of chondrogenesis. Despite the chondrogenic nature of sclera-derived cells, lack of cartilage in the sclera in humans may be attributed to cis- and trans-regulation of cartilage-associated gene(s), or an unclarified inhibitory mechanism that was altered during evolution (Fig. 4).

Implication of chondrogenic nature of sclera in diseases

The fact that the gene expression pattern of the human fibrous sclera is similar to that of cartilage is interesting not only as comparative anatomy but also from a patho-etiological view point. The sclera and the joint cartilage are common targets for inflammatory cells in rheumatic arthritis [22,23] or polychondritis [24], implying common proteins between the sclera and the synovium. Although the target protein(s) remains unclarified, our findings directly explain an enigma that both the sclera and the joint cartilage are affected in rheumatic arthritis. Furthermore, mutations in genes for type II and type XI collagen are a cause of Stickler syndrome [25,26]. Patients with Stickler syndrome have joint deformity and severe high myopia due to an abnormality of the sclera. These affected lesions may be attributed to the chondrogenic nature of human sclera. In conclusion, our present study shows a chondrogenic potential of human sclera and explains the etiology of scleral disorders, at least in part. In addition, we would like to emphasize that the first database of gene expression in the human infant sclera (uploaded to GEO accession #GSE10934 at http://www.ncbi.nlm.nih.gov/geo/index.cgi) may contribute to the elucidation of scleral diseases in the future.

Materials and Methods

Isolation and cell culture of human scleral cells

Scleral tissues were excised from surgical specimens as a therapy of retinoblastoma, under signed informed consent, with the approval (approval number, #156) of the Ethics Committee of the National Institute for Child and Health Development, Tokyo. Signed informed consent was obtained from donors, and the surgical specimens were irreversibly de-identified. All experiments handling human cells and tissues were performed in line with the Tenets of the Declaration of Helsinki. The scleral pieces were cut into smaller pieces and cultured in the growth medium (GM): Dulbecco's modified Eagle's medium (DMEM)/Nutrient mixture F12 (1:1) with high glucose supplemented with 10% fetal bovine serum, insulin-transferrin-selenium, and MEM-NEAA (GIBCO).

Oligonucleotide microarray

Total RNAs were isolated from cultured scleral cells in the growth medium without any induction of differentiation to perform the gene chip analysis. Total RNA was extracted from a total of 5×10^6 cultured human scleral cells and other mesenchymal cells (Table 1) using RNeasy Plus mini-kit® (Qiagen, Maryland, USA) according to

the manufacturer's instructions. A comprehensive expression analysis was performed using 2 μg of total RNA from each sample and GeneChip® Human Genome U133 plus 2.0 probe arrays (Affymetrix, Santa Clara, CA) according to the manufacturer's instructions. To normalize the variations in staining intensity among chips, the 'Signal' values for all probes on a given chip were divided by the median value for expression of all genes on the chip. To consider genes containing only a background signal, probes were eliminated only if the 'Signal' value was less than 10, or the Detection call was 'Absent' in any sample using GeneSpring software version 7.2 (Agilent Technologies, Palo Alto). The gene chip analysis was carried out on 8 independent scleral cultures.

Hierarchical clustering and principal component analysis (PCA)

To analyze the gene expression data in an unsupervised manner by gene chip array, we used hierarchical clustering and principal component analysis (NIA Array; http://lgsun.grc.nia.nih.gov/ANOVA/ [27], TIGR MeV; http://www.tm4.org/mer.html [28]). The hierarchical clustering techniques classify data by similarity and the results are represented by dendrogram. PCA is a multivariate analysis technique which finds major patterns in data variability. Hierarchical clustering and PCA were performed on the data of gene chip analysis (a single assay for each sample) to group scleral cells and other mesenchymal cells into subcategories (Table 1).

In vitro chondrogenesis

Two hundred thousand scleral cells were placed in a 15-ml polypropylene tube (Becton Dickinson) and centrifuged for 10 minutes. The pellet was cultured in DF-C medium™ containing 0.1 μM dexamethasone, 1 mM sodium pyruvate, 0.17 mM ascorbic acid-2-phosphate, 0.35 mM proline, 6.25 μg/ml bovine insulin, 6.25 μg/ml transferrin, 6.25 μg/ml selenous acid, 5.33 μg/ml linoleic acid, 1.25 mg/ml BSA, 5 ng/ml TGF-β1, 5 ng/ml BMP2, and 3% fetal bovine serum (TOYOBO). The medium was replaced every 3 to 4 days for 28 days. For microscopy, the pellets were embedded in paraffin, cut into 5-μm sections, and stained with alcian blue [29,30].

In vivo chondrogenesis

Under anesthesia, full thickness cartilage defects were created in the trochlear groove of the femur in SD rats. The defects were filled with DiI-labeled human scleral cells. The rats were returned to their cages after the operation and allowed to move freely. Animals were sacrificed with an overdose of sodium pentobarbital at 4 weeks after the operation. Specimens were dissected and embedded in paraffin. The sections were stained with toluidine blue and immunohistochemically stained with anti-type II collagen antibodies (clone F-57, DAIICHI FINE CHEMICAL, Co. Ltd., Toyama, Japan). All animals received humane care in compliance with the "Principles of Laboratory Animal Care" formulated by the National Society for Medical Research and the "Guide for the Care and Use of Laboratory Animals" prepared by the Institute of Laboratory Animal Resources and published by the US National Institutes of Health (NIH Publication No. 86-23, revised 1985). The operation protocols were accepted by the Laboratory Animal Care and Use Committee of the Research Institute for Child and Health Development (2003-002).

Reverse transcriptase-PCR

Total RNA was isolated with an RNeasy Plus mini-kit. Cartilage pellets were digested with 3 mg/ml Collagenase D for 3 hours at 37°C.

The following PCR primer sets were used for cartilage-associated genes: aggrecan, sense (5′-TACACTGGCGAGCACTGTAAC -3′) and antisense (5′-CAGTGGCCCTGGTACTTGTT-3′), product size, 71 bp; collagen, type II, alpha 1, sense (5′-TTCAGCTATG-GAGATGACAATC -3′) and antisense (5′-AGAGTCCTAGAGT-GACTGAG -3′), product size, 472 bp; collagen, typeX, alpha 1, sense (5′-CACCTTCTGCACTGCTCATC-3′) and antisense (5′-GGCAGCATATTCTCAGATGGA-3′), product sizem, 104 bp; SOX5, sense (5′-AGCCAGAGTTAGCACAATAGG -3′) and antisense (5′-CATGATTGCCTTGTATTC -3′), product size, 619 bp; SOX6, sense (5′-ACTGTGGCTGAAGCACGAGTC -3′) and antisense (5′-TCCGCCATCTGTCTTCATACC -3′), product size, 562 bp; SOX9, sense (5′-GTACCCGCACTTGCACAAC-3′) and antisense (5′-TCGCTCTCGTTCAGAAGTCTC-3′), product size 72 bp; Indian hedgehog homolog (IHH), sense (5′-TGCATTGCT-CCGTCAAGTC-3′) and antisense (5′-CCACTCTCCAGGCG-TACCT-3′), product size 88 bp; parathyroid hormone receptor 1(PTHR1), sense (5′-CCTGAGTCTGAGGAGGACAAG-3′) and antisense (5′-CACAGGATGTGGTCCCATT-3′), product size 86 bp; matrix metallopeptidase 13 (MMP13), sense (5′-CCAGTCTCC-GAGGAGAAACA-3′) and antisense (5′-AAAAACAGCTCCG-CATCAAC-3′),product size, 85 bp, and GAPDH, sense (5′-GCTCAGACACCATGGGGAAGGT-3′) and antisense (5′-GTGGTGCAGGAGGCATTGCTGA-3′), product size, 474 bp.

Supporting Information

Figure S1 Global gene expression analysis of cultured human cells. Hierarchical clustering analysis based on expression levels of the cartilage-associated genes (NIA Array Analysis). We performed gene chip analysis (a single assay for each analysis) for eight independent primary scleral cultures from five patients (donors). We started eight independent cultures from three different scleral sites of Donor 2 (e.g. the anterior site 1.5 mm apart from the limbs, the middle part, and the posterior part), 2 different scleral sites of Donor 5, and three scleral sites of Donor 1, 3, and 4. We performed hierarchical clustering analysis, using these independent cultures and obtained consistent results, that is, "sclera"-derived cells are categorized into one sub-group. Furthermore, the sclera, cartilage, synovium, and joint fluid are categorized into the same group.

Found at: doi:10.1371/journal.pone.0003709.s001 (0.07 MB PDF)

Figure S2 Cartilage-associated gene expressions in cultured fibroblasts derived from the dermis and the sclera. Cartilage-associated gene expressions by RT-PCR in cultured fibroblasts derived from the dermis and the sclera. Aggrecan, COL2A, IHH and PTHR mRNA expressions were clearly stronger in the scleral fibroblasts compared to the dermal fibroblasts, indicating that chondrogenic nature could be specific for the sclera among collagenous tissues.

Found at: doi:10.1371/journal.pone.0003709.s002 (0.01 MB PDF)

Table S1 Cartilage-associated genes

Found at: doi:10.1371/journal.pone.0003709.s003 (0.01 MB PDF)

Acknowledgments

We would like to express our sincere thanks to T. Tang for helping with animal experiments and T. Sugiki, M. Nasu, A. Kawakita and M. Toyoda for their discussion of this work.

Author Contributions

Conceived and designed the experiments: YS NA TM IS AU. Performed the experiments: YS NA HM TM IS. Analyzed the data: YS YT KM HS IS. Contributed reagents/materials/analysis tools: YS NA IS. Wrote the paper: YS KM HS IS AU.

References

1. Connon CJ, Meek KM, Kinoshita S, Quantock AJ (2004) Spatial and temporal alterations in the collagen fibrillar array during the onset of transparency in the avian cornea. Exp Eye Res 78: 909–915.
2. Yoshida S, Shimmura S, Shinozaki J, Shinozaki N, Tsubota K (2005) Serum-free spheroid culture of mouse corneal keratocytes. Invest Ophthalmol Vis Sci 46: 1653–1658.
3. Zhou J, Rappaport EF, Tobias JW, Young TL (2006) Differential gene expression in mouse sclera during ocular development. Invest Ophthalmol Vis Sci 47: 1794–1802.
4. Young TL, Guo XD, King RA, Johnson JM, Rada JA (2003) Identification of genes expressed in a human scleral cDNA library. Mol Vis 9: 508–514.
5. Sakaguchi Y, Sekiya I, Yagishita K, Muneta T (2005) Comparison of human stem cells derived from various mesenchymal tissues: superiority of synovium as a cell source. Arthritis Rheum 52: 2521–2529.
6. Yoshimura H, Muneta T, Nimura A, Yokoyama A, Koga H, et al. (2007) Comparison of rat mesenchymal stem cells derived from bone marrow, synovium, periosteum, adipose tissue, and muscle. Cell Tissue Res 327: 449–462.
7. Koga H, Muneta T, Ju YJ, Nagase T, Nimura A, et al. (2007) Synovial stem cells are regionally specified according to local microenvironments after implantation for cartilage regeneration. Stem Cells 25: 689–696.
8. Seko Y, Shimokawa H, Tokoro T (1995) Expression of bFGF and TGF-beta 2 in experimental myopia in chicks. Invest Ophthalmol Vis Sci 36: 1183–1187.
9. Seko Y, Tanaka Y, Tokoro T (1995) Influence of bFGF as a potent growth stimulator and TGF-beta as a growth regulator on scleral chondrocytes and scleral fibroblasts in vitro. Ophthalmic Res 27: 144–152.
10. Franz-Odendaal TA, Hall BK (2006) Skeletal elements within teleost eyes and a discussion of their homology. J Morphol 267: 1326–1337.
11. Archer CW, McDowell J, Bayliss MT, Stephens MD, Bentley G (1990) Phenotypic modulation in sub-populations of human articular chondrocytes in vitro. J Cell Sci 97 (Pt 2): 361–371.
12. Hauselmann HJ, Fernandes RJ, Mok SS, Schmid TM, Block JA, et al. (1994) Phenotypic stability of bovine articular chondrocytes after long-term culture in alginate beads. J Cell Sci 107 (Pt 1): 17–27.
13. Reginato AM, Iozzo RV, Jimenez SA (1994) Formation of nodular structures resembling mature articular cartilage in long-term primary cultures of human fetal epiphyseal chondrocytes on a hydrogel substrate. Arthritis Rheum 37: 1338–1349.
14. Benya PD, Shaffer JD (1982) Dedifferentiated chondrocytes reexpress the differentiated collagen phenotype when cultured in agarose gels. Cell 30: 215–224.
15. Bonaventure J, Kadhom N, Cohen-Solal L, Ng KH, Bourguignon J, et al. (1994) Reexpression of cartilage-specific genes by dedifferentiated human articular chondrocytes cultured in alginate beads. Exp Cell Res 212: 97–104.
16. Lefebvre V, Peeters-Joris C, Vaes G (1990) Production of collagens, collagenase and collagenase inhibitor during the dedifferentiation of articular chondrocytes by serial subcultures. Biochim Biophys Acta 1051: 266–275.
17. Pittenger MF, Mackay AM, Beck SC, Jaiswal RK, Douglas R, et al. (1999) Multilineage potential of adult human mesenchymal stem cells. Science 284: 143–147.
18. Shukunami C, Shigeno C, Atsumi T, Ishizeki K, Suzuki F, et al. (1996) Chondrogenic differentiation of clonal mouse embryonic cell line ATDC5 in vitro: differentiation-dependent gene expression of parathyroid hormone (PTH)/PTH-related peptide receptor. J Cell Biol 133: 457–468.
19. Lefebvre V, Li P, de Crombrugghe B (1998) A new long form of Sox5 (L-Sox5), Sox6 and Sox9 are coexpressed in chondrogenesis and cooperatively activate the type II collagen gene. Embo J 17: 5718–5733.
20. Sekiya I, Tsuji K, Koopman P, Watanabe H, Yamada Y, et al. (2000) SOX9 enhances aggrecan gene promoter/enhancer activity and is up-regulated by retinoic acid in a cartilage-derived cell line, TC6. J Biol Chem 275: 10738–10744.
21. Kobayashi T, Soegiarto DW, Yang Y, Lanske B, Schipani E, et al. (2005) Indian hedgehog stimulates periarticular chondrocyte differentiation to regulate growth plate length independently of PTHrP. J Clin Invest 115: 1734–1742.
22. Jayson MI, Jones DE (1971) Scleritis and rheumatoid arthritis. Ann Rheum Dis 30: 343–347.
23. Barr CC, Davis H, Culbertson WW (1981) Rheumatoid scleritis. Ophthalmology 88: 1269–1273.
24. Isaak BL, Liesegang TJ, Michet CJ Jr (1986) Ocular and systemic findings in relapsing polychondritis. Ophthalmology 93: 681–689.
25. Annunen S, Korkko J, Czarny M, Warman ML, Brunner HG, et al. (1999) Splicing mutations of 54-bp exons in the COL11A1 gene cause Marshall syndrome, but other mutations cause overlapping Marshall/Stickler phenotypes. Am J Hum Genet 65: 974–983.
26. Van Camp G, Snoeckx RL, Hilgert N, van den Ende J, Fukuoka H, et al. (2006) A new autosomal recessive form of Stickler syndrome is caused by a mutation in the COL9A1 gene. Am J Hum Genet 79: 449–457.
27. Sharov AA, Dudekula DB, Ko MS (2005) A web-based tool for principal component and significance analysis of microarray data. Bioinformatics 21: 2548–2549.
28. Saeed AI, Sharov V, White J, Li J, Liang W, et al. (2003) TM4: a free, open-source system for microarray data management and analysis. Biotechniques 34: 374–378.
29. Sugiki T, Uyama T, Toyoda M, Morioka H, Kume S, et al. (2007) Hyaline cartilage formation and enchondral ossification modeled with KUM5 and OP9 chondroblasts. J Cell Biochem 100: 1240–1254.
30. Sekiya I, Larson BL, Vuoristo JT, Reger RL, Prockop DJ (2005) Comparison of effect of BMP-2, -4, and -6 on in vitro cartilage formation of human adult stem cells from bone marrow stroma. Cell Tissue Res 320: 269–276.
31. Morito T, Muneta T, Hara K, Ju YJ, Mochizuki T, et al. (2008) Synovial fluid-derived mesenchymal stem cells increase after intra-articular ligament injury in humans. Rheumatology (Oxford) 47: 1137–1143.
32. Segawa Y, Muneta T, Makino M, Nimura A, Mochizuki T, et al. (in press) Mesenchymal stem cells derived from synovium, meniscus, anterior cruciate ligament, and articular chondrocytes share similar gene expression profiles. Journal of Orthopaedic Research.
33. Tsuruga Y, Kiyono T, Matsushita M, Takahashi T, Kasai N, et al. (2008) Effect of intrasplenic transplantation of immortalized human hepatocytes in the treatment of acetaminophen-induced acute liver failure SCID mice. Transplant Proc 40: 617–619.
34. Mochizuki T, Muneta T, Sakaguchi Y, Nimura A, Yokoyama A, et al. (2006) Higher chondrogenic potential of fibrous synovium- and adipose synovium-derived cells compared with subcutaneous fat-derived cells: distinguishing properties of mesenchymal stem cells in humans. Arthritis Rheum 54: 843–853.

RBM Online - Vol 16 No 1. 2008 41-50 Reproductive BioMedicine Online; www.rbmonline.com/Article/3061 on web 13 November

Symposium: Nuclear reprogramming and the control of differentiation in mammalian embryos

Elucidating nuclear reprogramming mechanisms: taking a synergistic approach

Dr Hidenori Akutsu became interested in nuclear reprogramming in mammalian species when he was a research fellow at University of Hawaii under Dr Ryuzo Yanagimachi. This interest endured and motivated him to undertake further research under Dr Minoru Ko at NIA/NIH (embryo genomics) and Dr Kevin Eggan at Harvard University (epigenetic and nuclear reprogramming). While at Harvard University he also became an important part of Dr Douglas Melton's team, deriving human embryonic stem cell lines which were later offered freely to the scientific community to facilitate the efforts of other scientists. His special interests are egg development, epigenetic and nuclear reprogramming and embryonic stem cells.

Dr Hidenori Akutsu

Stephen Sullivan[1,3], Justin K Ichida[1], Akihiro Umezawa[2], Hidenori Akutsu[2]
[1]Stowers Medical Institute and Harvard Stem Cell Institute, Department of Cellular and Molecular Biology, Harvard University, 7 Divinity Avenue, SF457, Cambridge 02138, USA; [2]National Research Institute for Child Health and Development Department of Reproductive Biology and Pathology 2-10-1 Okura, Setagaya, Tokyo 157-8535, Japan
[3]Correspondence: e-mail: sullivan@mcb.harvard.edu.

Abstract

Nuclear reprogramming is the process by which a differentiated somatic nucleus has developmental potential restored to it. It involves heritable changes in gene expression as well as structural and functional changes to chromatin structure. This process is naturally induced immediately after fertilization, but can also be artificially induced by nuclear transfer, cell fusion and also now by viral transduction with four stem cell genes. However, the frequency of successful reprogramming is low in each system. The highest success rates, those using nuclear transfer, are only of the order of 2–5%. This article briefly reviews these three methods and proposes a synergistic approach where conditions that facilitate reprogramming in one system are transposed to the others. This might increase the incidence of successful reprogramming and identify common steps necessary for the reacquisition of developmental potential.

Keywords: *developmental potential, differentiation, embryonic stem cell, nuclear reprogramming, nuclear transfer, pluripotency*

Cell differentiation and nuclear reprogramming

Cell differentiation is the process by which a cell becomes specialised to perform specific biological functions (Gurdon, 1968). The process is associated with a decline in the range of cell types that the cell is capable of generating (Gurdon, 1968). It had been initially thought that as cells differentiated, hereditary material no longer required was cast off or permanently inactivated (Weismann, 1893). However, this paradigm was shown to be false more than 50 years ago when Briggs and King transferred differentiated nuclei from blastula cells to enucleated eggs of the frog *Rana pipiens* (Briggs and King, 1952). These reconstructed cells went on to generate normal hatched embryos, showing that nuclei of differentiated cells contain the same genetic material as those of undifferentiated cells. The current paradigm for how cell differentiation occurs involves the assembly of condensed chromosomal structures (Kass and Wolffe, 1998). Such structures, formed via interactions between DNA and protein, are thought to compartmentalize chromatin into functional domains and, in some unknown way, stably maintain the differentiated state even when the cell divides.

In terms of mammalian development, differentiation first occurs at the blastocyst stage in the preimplantation embryo. As the embryo develops, the outer layer cells of the embryo (the trophectoderm) become morphologically distinct from the inner cell mass (ICM). Cells of the trophectoderm and ICM have different developmental potentials, e.g. cells of the ICM have the potential to form all the cells of the conceptus, whereas the trophectoderm cells have only the potential to form extraembryonic cells or the placenta.

The processes responsible for the epigenetic changes that lead to dedifferentiation are referred to as nuclear reprogramming mechanisms (Rideout *et al.*, 2001). Nuclear reprogramming in this sense refers to the process by which a specialized nucleus re-acquires developmental capacity. This definition includes complete reprogramming to a totipotent state (verifiable only by generation of viable offspring) and also partial reprogramming where pluripotency (the capacity to generate cells representative of all three germ layers) is restored. By necessity, it involves heritable changes to gene expression, i.e. changes in gene expression that are passed on to daughter cells. Some have suggested that transient changes to gene expression constitute nuclear reprogramming (Hakelien *et al.*, 2002), but such changes do not persist, nor is there any evidence that they are transferred to progeny cells. Such observations almost certainly result from residual transcription activity rather than the consequence of a reprogrammed genome, and so these examples do not constitute nuclear reprogramming as defined here and elsewhere (Hochedlinger and Jaenisch, 2006).

Naturally induced nuclear reprogramming

The differentiated state of cells is found to be extremely stable (Kato and Gurdon, 1993). The only stage during which normal mammalian cells seem to naturally dedifferentiate immediately follows fertilization (Schultz *et al.*, 1999). The sperm and oocyte, both highly differentiated cells with condensed chromatin structure, fuse to produce a zygote. Within the zygote, changes lead to the reversion to a less specialised totipotent cellular state (Kelly, 1977). Although the mechanism responsible is unknown, two events are associated with this dedifferentiation: chromatin structure becomes less dense: protamines are removed from sperm-derived chromatin and replaced by oocyte-derived histones (Perreault, 1992); and methylated haploid parental genomes are demethylated (Barton *et al.*, 2001).

Additionally, it has been speculated that inappropriate or incomplete nuclear reprogramming may occur in a pathological context, i.e. during the generation of teratomas. Teratomas are benign tumours associated with chaotic cell-lineage formation. The 'dedifferentiation' theory of cancer states that such lineages may arise from cells that have undergone dedifferentiation to a multipotent state (Ribbert, 1911). Teratomas can also be produced experimentally by injection of pluripotent stem cells into ectopic sites of a syngeneic animal (Evans and Kaufman, 1981; Matsui *et al.*, 1992; Rensnick *et al.*, 1992), so it is conceivable that inappropriately reprogrammed somatic cells could be the origin of such cancers.

Artificially induced nuclear reprogramming

In non-transformed somatic cells, once the differentiation programme of a cell has started, the process is normally irreversible. However, this programme may be reversed artificially. Using nuclear transfer (NT) (Wilmut *et al.*, 1997), cell fusion (Tada *et al.*, 1997), or even viral transduction of four specific stem cell genes (Takahashi and Yamanaka, 2006), it is possible to artificially and heritably alter a cell's gene expression and its functional identity. These techniques are collectively termed 'artificial induction of nuclear reprogramming' (**Figure 1**). The conversion of differentiated cells to pluripotent cells illustrates that cells do not permanently lose the ability to be pluripotent during differentiation.

Frustratingly, the mechanism by which a somatic nucleus may be reprogrammed remains unknown, aside from the fact that such a mechanism almost certainly involves both structural (Kikyo *et al.*, 2000) and chemical (Monk *et al.*, 1987) changes to chromatin. It may be possible for human somatic cells to be reprogrammed to a pluripotent state. If successful, this strategy would provide a potentially endless source of cells for biological research, as well as medical applications (Stojkovic *et al.*, 2005; Verlinsky *et al.*, 2005), toxicity assessment, drug testing and possibly even gene therapy (Wobus and Boheler, 2005). **Figure 2** illustrates how identification of reprogramming molecules and mechanisms could facilitate cell replacement therapy in humans. Over the past century, organ transplantation has evolved rapidly to the current widespread use of donated organs for the treatment of end-stage kidney, heart, and liver failure. However, with limited supplies of organs and an increasing demand for them, many patients who need transplants do not receive them (Gridelli and Remuzzi, 2000). The increasing gap between supply and demand for tissue and organ transplants means that harnessing nuclear reprogramming mechanisms is important (Sullivan and Eggan, 2007).

Nuclear transfer: the oldest and still the most reliable reprogramming technique

Spemann (1938) originally suggested transplantation of nuclei between cells as a technique to study the role of genetic material in cellular differentiation. In nuclear transfer, the nucleus from a differentiated donor cell is transplanted into an enucleated oocyte. The oocyte can reprogramme even an adult differentiated nucleus and the new cell can develop as an embryo. Artificially induced nuclear reprogramming by NT was first demonstrated by Briggs and King in 1952, when they showed that transfer of somatic nuclei to enucleated eggs can direct development so that tadpoles are generated (Briggs and King, 1952). Gurdon later refined the technique so that adult and fertile frogs could be generated (Gurdon *et al.* 1958). Decades later, the production of 'Dolly', the first viable mammal derived by reprogramming a fully differentiated adult somatic cell, illustrated that the mammalian nuclear genome can be completely reprogrammed and totipotency of the nucleus restored (Wilmut *et al.*, 1997). The nuclei of these offspring contain genomes of identical sequence to that of the nuclear donor. At present, nuclear transfer is the only technique in which one can accomplish total nuclear reprogramming in an unequivocal manner; by deriving viable offspring from a reconstituted embryo. More recently, embryonic stem (ES) cells have been derived from cloned mice (Wakayama *et al.*, 2001). The ES cells produced by somatic cell nuclear transfer retained self-renewal and pluripotent features, contributing to all germ layers, including the germline. In addition, gene expression profiling experiments showed the ES cell lines derived from cloned and fertilized mouse blastocysts are indistinguishable (Brambrink *et al.*, 2006). The NT–ES cells are developmentally and functionally equivalent to the fertilization-derived ES cells.

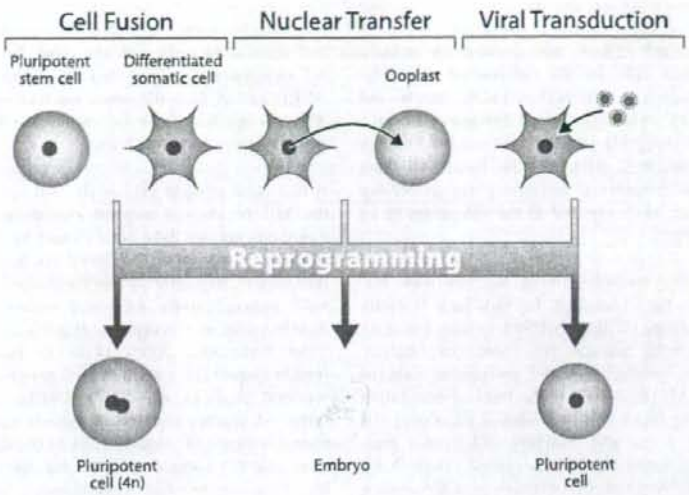

Figure 1. Artificially induced nuclear reprogramming. Cell fusion: a somatic cell fused with a pluripotent stem cell can be reprogrammed in the hybrid cell. These fused hybrid cells show similar features as embryonic stem (ES) cells; however the hybrid cell has a tetraploid karyotype and is unable to contribute to chimeras. Nuclear transfer: an adult somatic cell is transferred into an enucleated oocyte followed by artificial activation. These nuclear-transferred embryos can produce ES cells which are pluripotent, contributing to all germ layers including the germ cell lineage. Viral transduction: a somatic cell transduced by retroviruses expressing four key genes, *Oct3/4, Sox2, Klf4* and c-*Myc*, can be reprogrammed into iPS cells resembling ES cells in a cell-autonomous fashion. Only the nuclear transfer method can produce viable animals as it can return an adult nucleus to a totipotent, embryonic state.

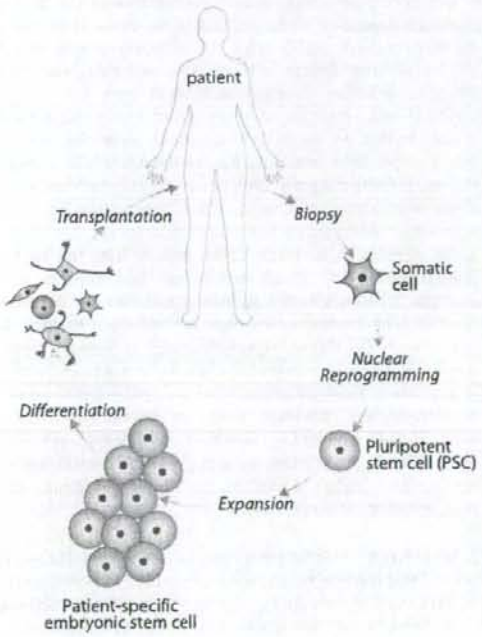

Figure 2. The ultimate goal of nuclear reprogramming research: controlled restoration of developmental potential. Once the mechanism by which nuclear reprogramming is understood, human somatic cells could be induced to dedifferentiate into pluripotent stem cells (PSC). PSC could then be expanded in culture and induced to redifferentiate into the cell type(s) required by the patient. These non-allogenic differentiated cells could then be transplanted into the patient with a decreased risk of immunorejection. It is also important to point out that patient matched pluripotent stem cells can also serve as in-vitro models for studying human disease and development at a cellular and molecular level. Such reprogramming will also allow the generation of genetically matched ES cells will, in themselves, provide scientists and clinicians an important new tool to recapitulate onset of specific diseases *in vitro* (Di Giorgio *et al.*, 2007).

Successful reprogramming of somatic nuclei by placing them in enucleated oocytes should perhaps not have been completely unexpected. There are compelling reasons why a system should exist for the removal of epigenetic modifications (excluding gametic imprints) in the oocytes and sperm. They are both highly specialized differentiated cells, and removal of their epigenetic patterns is essential to allow development of pluripotent cells from the inner cell mass (ICM). The same mechanism may be causing reprogramming of a somatic nucleus when exposed to the cytoplasm of an oocyte (Surani, 1999).

Many variables affect reprogramming success with NT. Some of these have been identified, i.e. structural integrity of the nuclear membrane (Willadsen 1986), quality and copy number of donor genetic material, chromatin conformation, histone composition, methylation and acetylation patterns (Campbell, 1999). Also important is the level of maturation or mitosis promoting factor (MPF) (Fulka *et al.*, 1996) and synchronization of donor and recipient cell cycles prior to embryo reconstruction (Campbell, 1996). High MPF concentrations in the oocyte and appropriate synchronization of donor and nuclear cell cycle using serum starvation are thought to minimize chromosomal damage and promote generation of reconstructed embryos that divide to produce normal diploid daughter cells.

Campbell suggests that the frequency of live offspring generation from reconstructed mammalian embryos made by NT is improved when the donor nuclei are in a quiescent state (Campbell *et al.*, 1996; Campbell, 1999). The successful production of Dolly, the first viable animal to be generated by nuclear transfer, used a nucleus from a cultured adult-differentiated somatic cell that had been serum starved into quiescence (Wilmut *et al.*, 1997). Kato *et al.* (1998) reported cloning of calves at 80% success ratio based on the number of transferred embryos using quiescent cumulus cells and oviduct epithelial cells that were cultured for several passages followed by serum starvation. Alternatively, using non-cultured cells also succeeded in producing cloned animals. Wakayama *et al.* (1998) used mouse cumulus cells, a naturally quiescent cell population, as nuclear donating cells in successful nuclear transfer experiments with mouse ooplasts. Ogura *et al.* (2000) made cloned mice by transferring Sertoli cells into enucleated mature oocytes. In both of these experiments, the cell cycle stage of the nuclear donors was controlled but the possibility that animals can be generated using non-quiescent cells as nuclear donors cannot be dismissed. Other researchers claim successful generation of mammalian offspring from nuclei not intentionally induced into a quiescent state (Cibelli *et al.*, 1998). Also, the possibility that transferred nuclei in Wakayama's and Ogura's experiments were non-quiescent cannot be eliminated.

Presumably, the importance of the state of the donor nucleus cell cycle is directly linked to compatibility with the recipient oocyte cytoplasm. Metaphase of second meiotic division (MII) oocytes has typically become the state of choice of recipient cytoplasts for NT procedures (Campbell *et al.*, 1996). MII oocytes contain active MPF to induce nuclear envelope breakdown (NEBD), premature chromosome condensation (PCC), and dispersion of nucleoli in the transferred nucleus, which may be essential for nuclear reprogramming. The donor nucleus in S phase of the cell cycle is likely to be incompatible with a high MPF state, leading to DNA damage and arrest at an early cleavage stage. However, inter-species NT experiments suggest that the occurrence and extent of NEBD and PCC in the donor nucleus are variable between different species, donor cell types and different procedures (Meissner and Jaenisch, 2006).

It had been thought previously that only the cytoplasm of the MII oocyte can support reprogramming after NT, so numerous species have been cloned by NT into MII oocyte (Meissner and Jaenisch, 2006). It seemed necessary for initiating reprogramming that the donor nucleus had elevated MPF concentrations, since NT embryos fail to develop, transforming into interphase zygotes (McGrath and Solter, 1984; Wakayama, 2000). However, more recently, a new insight disproving a myth of MII necessity for NT has been reported (Egli *et al.*, 2007). Unlike interphase zygotes, fertilized zygotes arrested in mitosis can fully support the reprogramming of somatic cells to the totipotent state. This indicates that factors sufficient for reprogramming are not limited to oocytes, and suggests that a continuum of activity extends beyond the unfertilized egg (Egli *et al.*, 2007). Why is the metaphase cell useful for reprogramming? A possible explanation is that condensed chromatin expels transcription factors like Oct-3/4 and Sox2 (Martinez-Balbas *et al.*, 1995), and without a nuclear membrane to enclose them, they are free to interact with any foreign chromatin introduced. Also, as the cell is poised to divide in M phase, it has synthesized many components of the cell to elevated levels, so presumably factors necessary for reprogramming are present in a greater abundance than at other stages of the cell cycle.

Experiments by Eggan *et al.* (2001) show that the number of live mice generated from cells reprogrammed via nuclear transfer is dependent on the genetics of the mouse from which the nuclear donor cell is taken. ES cells taken from inbred 129/SvJae mice fail to produce any post-natal surviving offspring, whereas cloned pups derived from ES cells of C57BL/6 and 129/SvJae matings can survive to adulthood. It may be that the use of inbred animals as nuclear donors introduces a reprogramming barrier not present in hybrids strains. Investigating why this occurs might elucidate more about mechanisms involved in nuclear reprogramming.

Much remains to be learnt about how somatic nuclei are reprogrammed after being transferred into ooplasts. For example, what factors and signalling pathways are involved in altering the chromatin structure, methylation patterns, and gene expression during reprogramming? Is there a master trigger that induces a cascade of downstream events or does it take several factors working in parallel pathways to initiate reprogramming? This might be the case as the frequency of successful reprogramming is so low. How do subtle epigenetic differences from normal animals, such as methylation/acetylation patterns, contribute to the abnormalities that cloned animals often exhibit?

In summary, successful production of cloned animals by NT proved that somatic nuclei could reverse their developmental clock to recreate totipotency in the oocyte. The transferred nuclei must be reprogrammed in resetting of an embryonic transcriptional programme. Although NT remains the tool